DIVISION OF CONSTRUCTION AND RESEARCH

TRANSPORTATION LABORATORY

RESEARCH REPORT

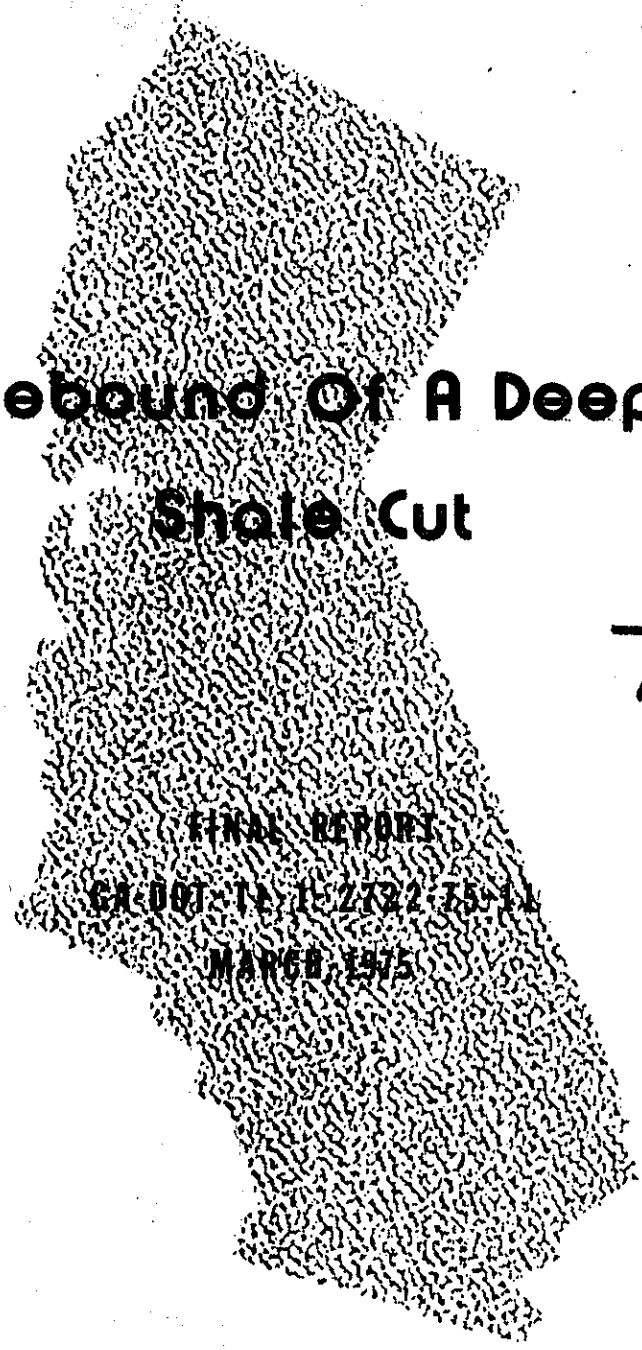

Rebound Of A Deep Shale Cut

75-11

FINAL REPORT

CA-DOT-TL-2732-75-11

MARCH 1975

Prepared in Cooperation with the U.S. Department of Transportation,

Federal Highway Administration

Caltrans

CALIFORNIA DEPARTMENT OF TRANSPORTATION

TECHNICAL REPORT STANDARD TITLE PAGE

1. REPORT NO.	2. GOVERNMENT ACCESSION NO.	3. RECIPIENT'S CATALOG NO.

4. TITLE AND SUBTITLE
REBOUND OF A DEEP SHALE CUT

5. REPORT DATE
March 1975

6. PERFORMING ORGANIZATION CODE
19202-762503-632722

7. AUTHOR(S)
Forsyth, R. A., Smith, R. E., Cortright, D. J.

8. PERFORMING ORGANIZATION REPORT NO.
CA-DOT-TL-2722-1-75-11

9. PERFORMING ORGANIZATION NAME AND ADDRESS
Transportation Laboratory
5900 Folsom Boulevard
Sacramento, California 95819

10. WORK UNIT NO.

11. CONTRACT OR GRANT NO.
D-5-10

12. SPONSORING AGENCY NAME AND ADDRESS
California Department of Transportation
Division of Construction and Research
Sacramento, California 95807

13. TYPE OF REPORT & PERIOD COVERED
Final

14. SPONSORING AGENCY CODE

15. SUPPLEMENTARY NOTES
Work plan title in cooperation with the U. S. Department of Transportation, Federal Highway Administration

16. ABSTRACT

A research investigation was conducted of earth movements resulting from a deep highway cut in the Ridge Route shale formation (located 40 miles north of Los Angeles). Subsurface benchmarks and extensometers were used to measure vertical and horizontal rebound of the bottom and sides of the cut. Laboratory and field tests were run on material sampled to determine values of elastic moduli. Estimates of rebound using the Westergaard model were compared with measured rebound. Results were inconclusive due to problems in establishing boundary conditions for determining analysis of an infinite elastic system.

17. KEY WORDS	18. DISTRIBUTION STATEMENT
Earth movements, rebound, field measurement, laboratory tests, modulus of elasticity	Unlimited

19. SECURITY CLASSIF. (OF THIS REPORT)	20. SECURITY CLASSIF. (OF THIS PAGE)	21. NO. OF PAGES	22. PRICE
Unclassified	Unclassified	75	

HMRT – 1242 (ORIG. 9/72)

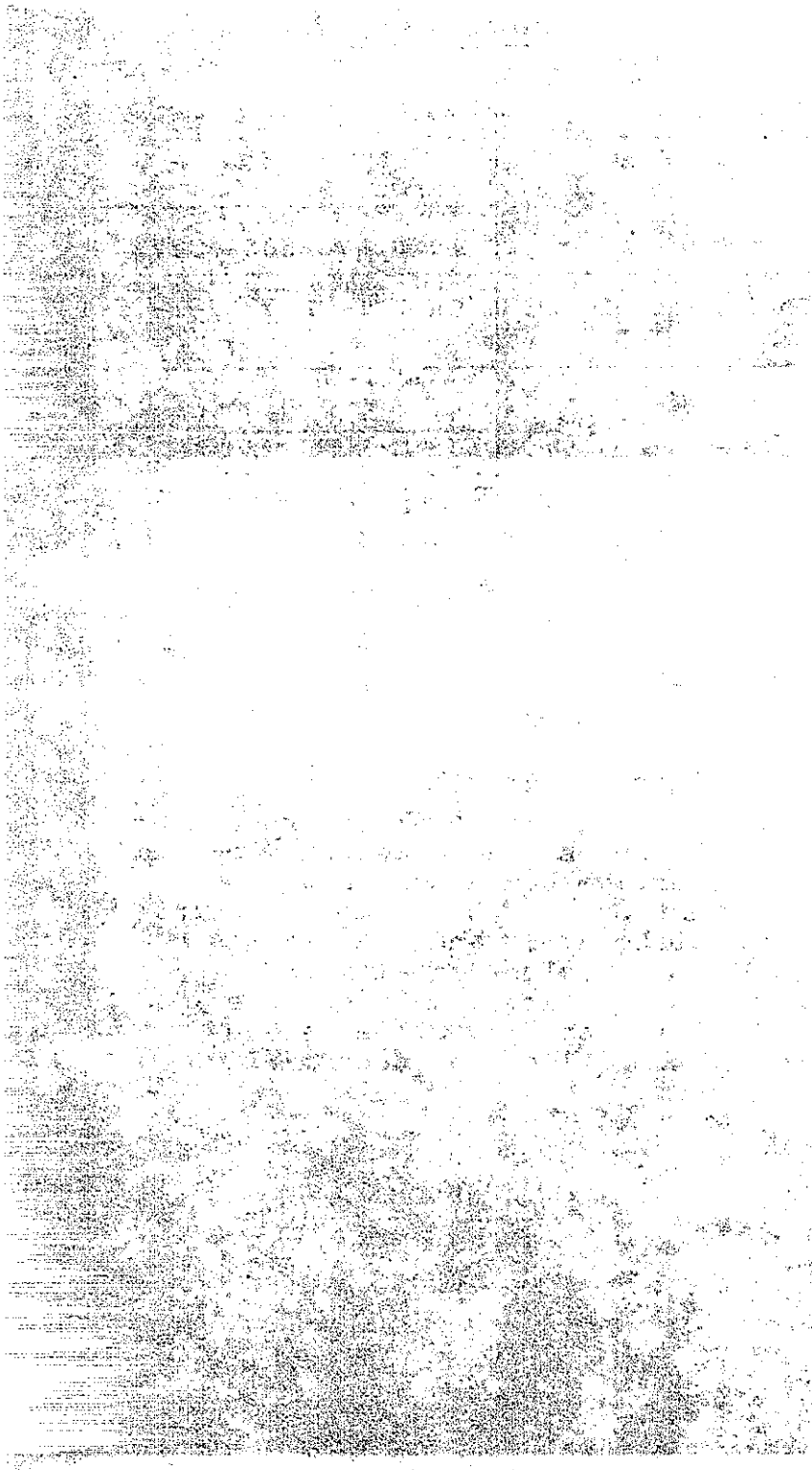

STATE OF CALIFORNIA
DEPARTMENT OF TRANSPORTATION
DIVISION OF CONSTRUCTION AND RESEARCH
TRANSPORTATION LABORATORY

March 1975

FHWA No. D-5-10
TL No. 632722

Mr. R. J. Datel
Chief Engineer

Dear Sir:

I have approved and now submit for your information this final research report titled:

REBOUND OF A DEEP SHALE CUT

Study made by . . . . . Geotechnical Branch

Under the Supervision of . . . . . Raymond A. Forsyth, P.E.

Principal Investigator . . . . . Donald L. Durr, P. E.

Analysis and Report by . . . . . Robert E. Smith, P. E.
and
Donald J. Cortright

Assisted by . . . . . D. W. Sathre
and
D. J. Hinrichs

Very truly yours,

JOHN L. BEATON
Chief Engineer, Transportation Laboratory

Attachment

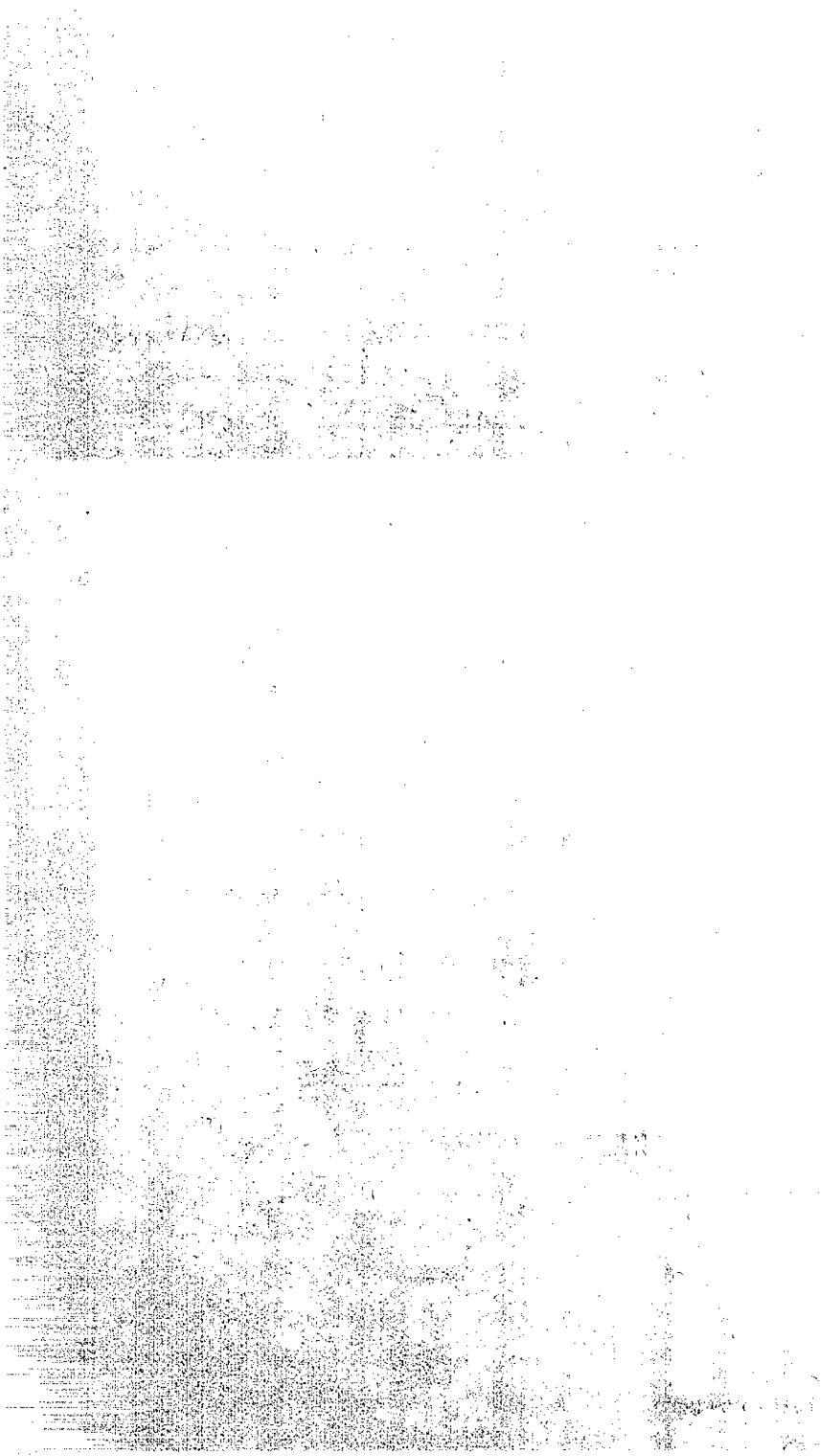

ACKNOWLEDGEMENT

The work reported herein was performed under research project TL No. 632722, titled, "Rebound of Materials in Highway Cuts". It was financed by Federal and HPR 1-1/2 percent funds, authorized under 1965-66 work program HPR 1(2) and 1(3), in cooperation with the U. S. Department of Transportation, Federal Highway Administration.

Appreciation is extended to the personnel of District 07 of the California Department of Transportation who contributed greatly to the project.

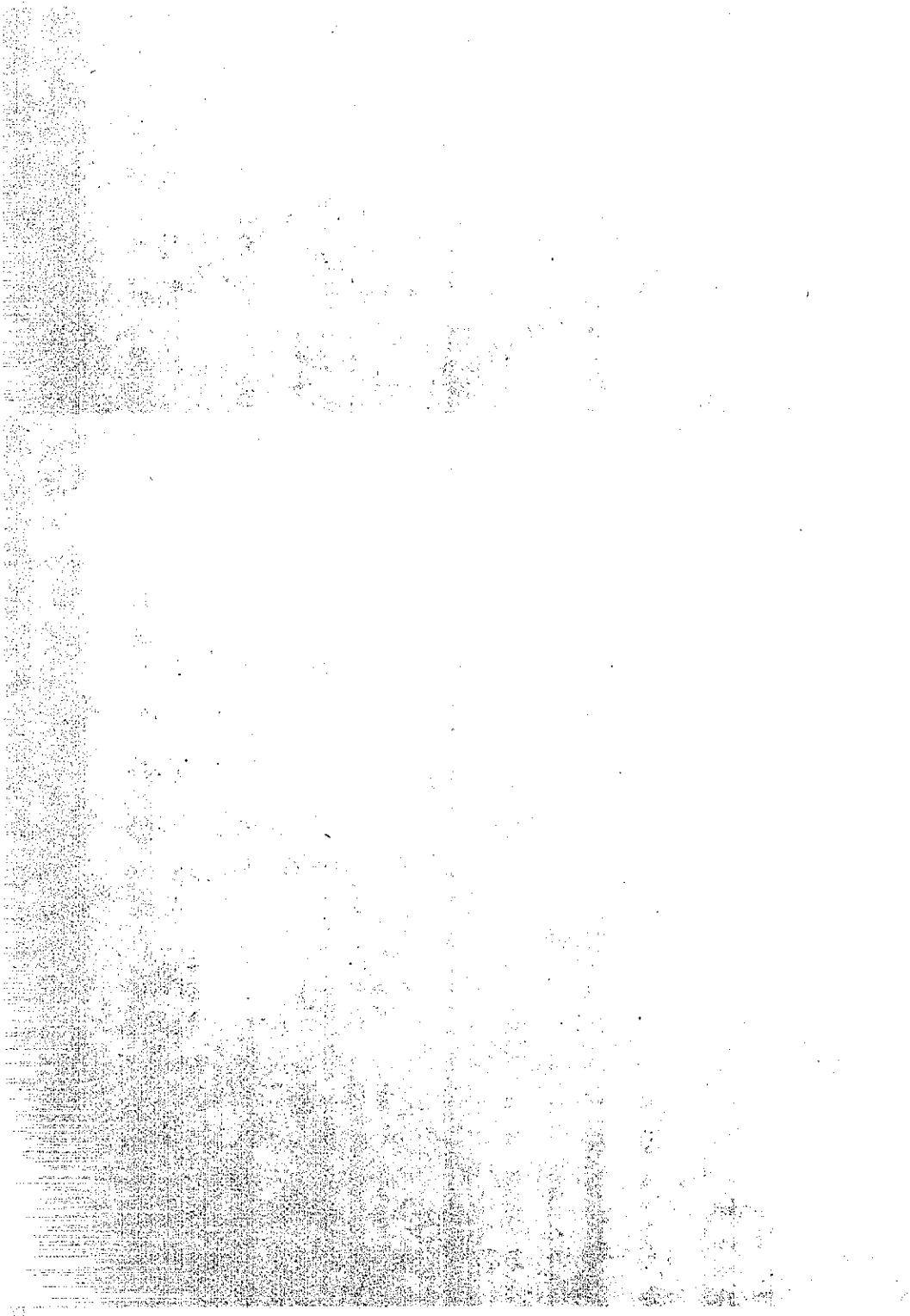

TABLE OF CONTENTS

	Page
ACKNOWLEDGEMENTS	i
LIST OF FIGURES	iv
LIST OF TABLES	vi
LIST OF PHOTOGRAPHS	vii
INTRODUCTION	1
CONCLUSIONS	2
RECOMMENDATIONS AND IMPLEMENTATION	3
LITERATURE SURVEY OF REBOUND MEASUREMENT AND ANALYSIS	4
1. Rebound of Shallow Excavations	4
2. Rebound of Excavations for Dams	5
3. Effects of Stress History, Field and Laboratory Observations	8
RESEARCH PROJECT	12
1. Proposal	12
2. Geology	13
3. Movement During and After Excavation of Cut	14
a. Subsurface Benchmarks	14
b. Water Level Device	14
c. Rebound of Subsurface Benchmarks	14
d. Extensometers	15
4. Seismic and Borehole Strength Testing	19
a. Seismic Survey	19
b. Menard Pressuremeter	20

TABLE OF CONTENTS (Cont.)

		Page
5.	Laboratory Testing of Shale Samples	20
	a. Description of Testing Program	20
	b. Consolidometer Stress-Strain Tests	21
	c. Unconfined Compression Tests	23
6.	Modulus Calculations	25
	a. E_p, Pressuremeter Modulus	25
	b. E_c, Consolidometer Modulus	26
	c. E_h, Unconfined High-Stress Compression Modulus	28
	d. E_s, Seismic Velocity Modulus	29
7.	Rebound Analysis by the Finite Element Method	30
8.	Rebound Analysis by Westergaard, Boussinesq Stress Distributions - Incremental Approximation	31
	Sample Calculation for the Effect of Removal of Layer Number 4 - Westergaard Stress Distribution	
9.	Comparison of Finite Element and Approximate Analyses	35
REFERENCES		38
FIGURES		41
TABLES		42
PHOTOGRAPHS		65

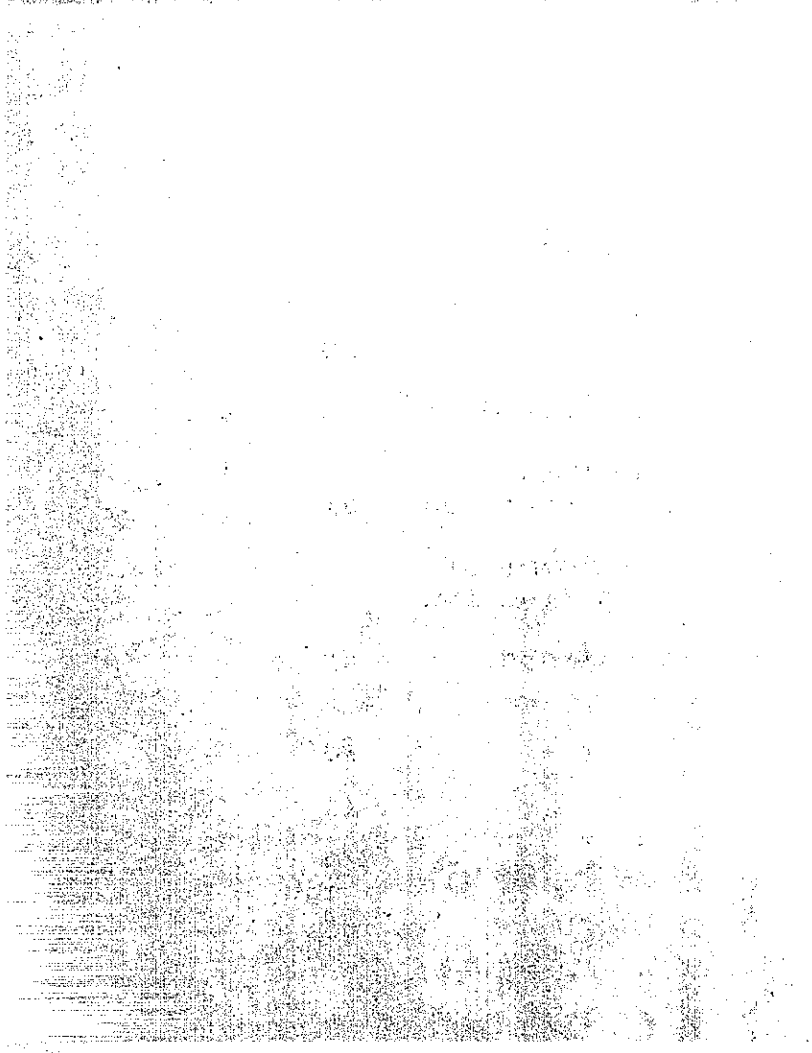

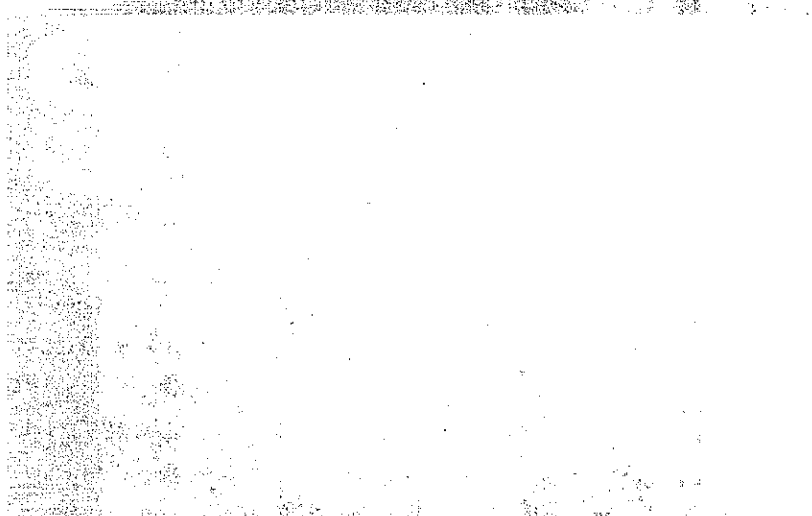

LIST OF FIGURES

Figure		Page
1	Location Map	42
2A	Plan View of Excavation	43
2B	Approximate Cross-Section	43
3	Structural Section Through Ridge Basin	44
4	Boring Profile, Sta. 64+50	45
5	Rebound vs. Cut Depth	46
6	Extensometer Movement vs. Time, Extensometers No. 1, 2 and 4	47
7	Extensometer Movement vs. Time, Extensometer No. 3	48
8	Extensometer Movement vs. Time, Extensometer No. 5	49
9	Extensometer Movement vs. Time, Extensometers No. 6, 7, 8 and 9	50
10	Extensometer Movement vs. Time, Extensometer No. 10	51
11	Extensometer Movement vs. Time, Extensometers No. 11, 12 and 14	52
12	Extensometer Movement vs. Time, Extensometer No. 13	53
13	Extensometer Movement vs. Time, Extensometers No. 15 and 17	54
14	Extensometer Movement vs. Time, Extensometer No. 16	55
15	Schematic of Menard Pressuremeter	56
16A	Menard Pressuremeter Data, Extensometer Boring No. 17	57
16B	Menard Pressuremeter Data, Extensometer Boring No. 16	57

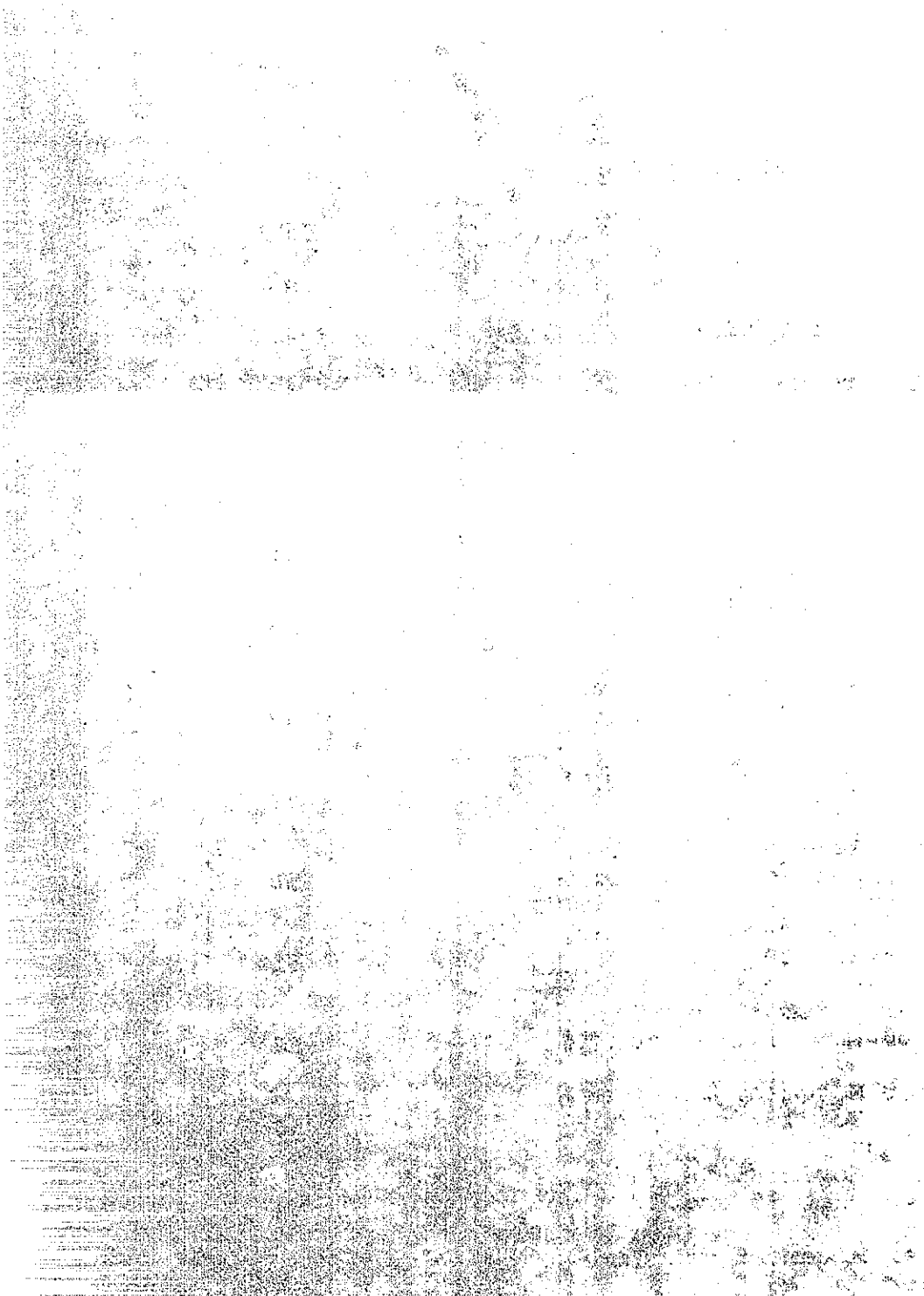

LIST OF FIGURES (Cont.)

Figure		Page
17	Stress vs. Strain, Confined Consolidometer Tests	58
18	Stress vs. Strain, Confined and Unconfined Consolidometer Tests	59
19	Stress vs. Strain, High Stress Unconfined Compression Tests	60
20	Moduli vs. Peak Stress	61
21	Actual and Assumed Excavation Limits for Finite Element Analysis of Rebound	62
22	Boundaries Assumed in the Finite Element Analysis of Rebound	63
23	Westergaard Stress Distribution for Long Continuous Load	64

Page

58

60

64

LIST OF TABLES

Table		Page
1	Estimate of Soil Minerology in Percent By X-Ray Diffraction and Differential Thermal Analysis	41

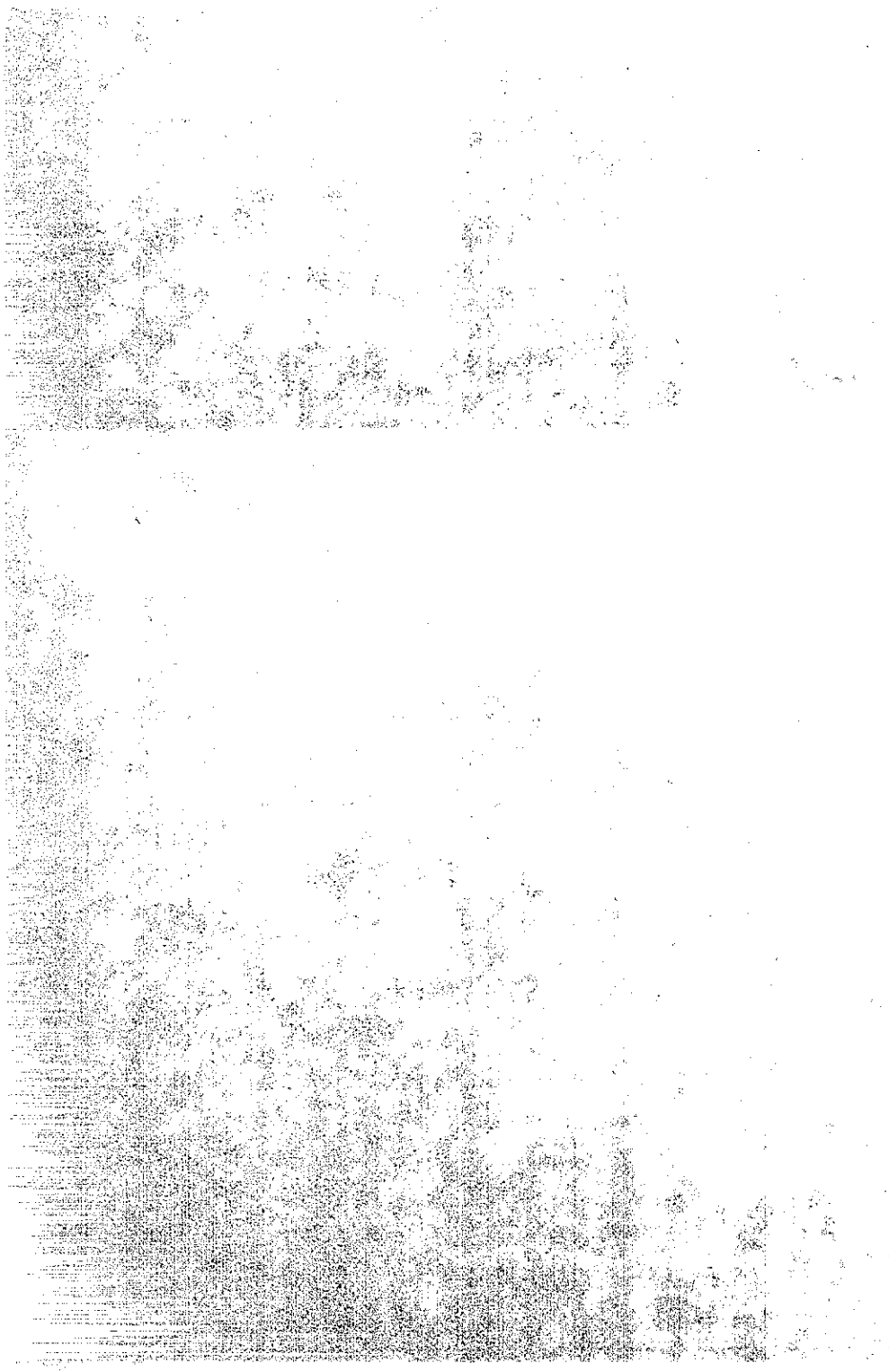

LIST OF PHOTOGRAPHS

Photo		Page
1	Westerly Face of Cut November 1967, 9 Months After Completion	65
2	Westerly Face of Cut March 1970 (Perspective is from the South)	65
3	Recovery of Extended Benchmark	66
4	Close-Up of Upper Benchmark at Time of Recovery	66
5	Exposed End of Extensometer With Dial Gage in Reading Position	67
6	Anchor End of Extensometer Made From Rock Bolt	67

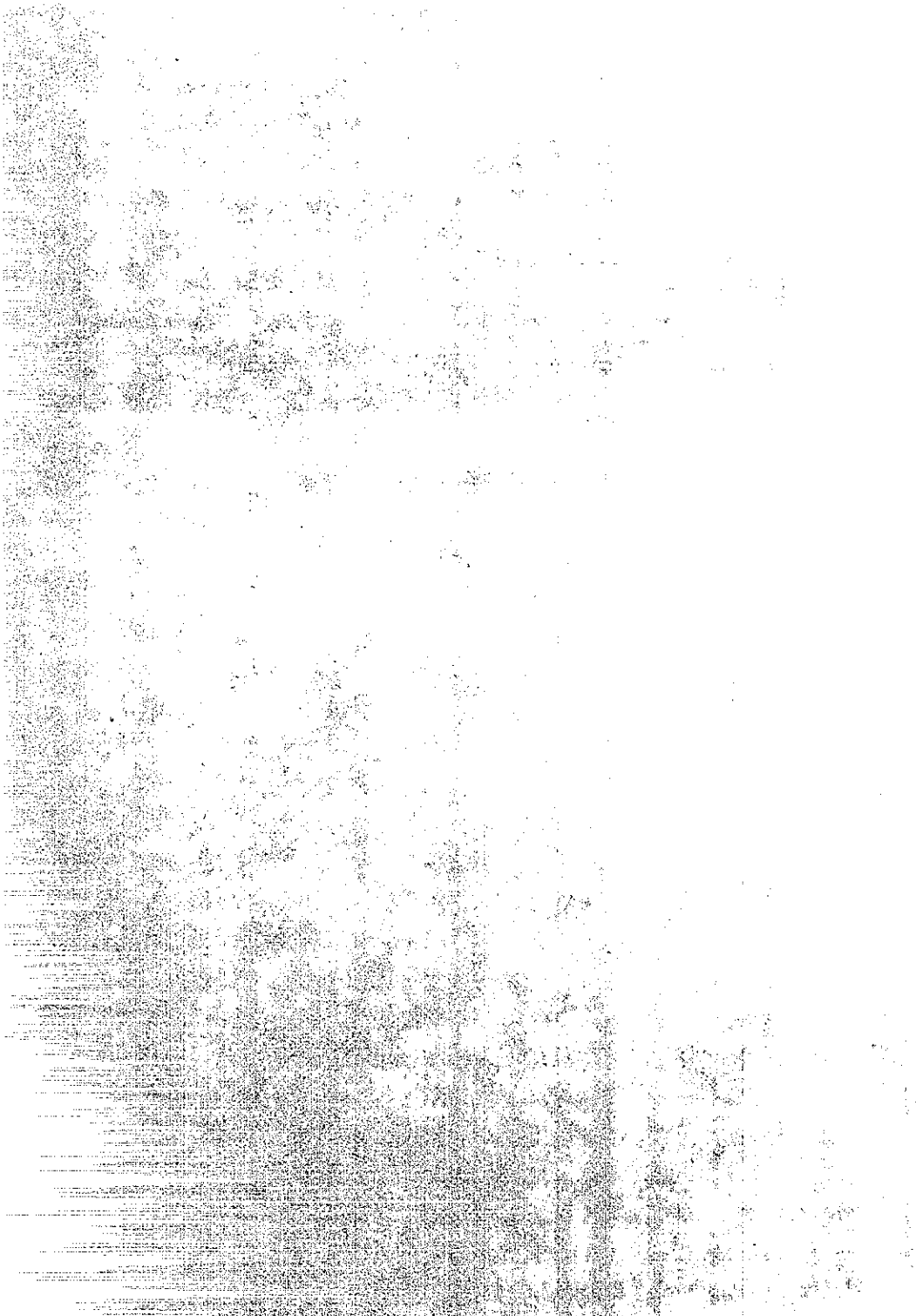

INTRODUCTION

The purposes of this research project were: (1) to evaluate earth movements which occur during and after deep excavation and (2) to implement, if warranted, modification in highway design and construction. This report presents the results of an investigation of the rebound accompanying a 260± foot cut in the Ridge Route shale on Route 07-LA-5, about 40 miles north of Los Angeles, and the subsequent analysis of data.

Subsurface benchmarks were placed to measure vertical movement of the cut bottom, and horizontal extensometers were used in the cut faces to monitor movement in the first 50 feet of depth. Seismic refraction surveys of the material were run. A description of the site, project history and results of field and laboratory work are reported. Slide movement at one location is also shown.

Elastic theory was adopted as a basis for estimating rebound using modulus of elasticity values computed from consolidometer, pressuremeter, seismic, and unconfined compressive strength tests. These moduli were used with Westergaard and finite element models for stress distribution in a nonisotropic elastic material to estimate the shale rebound.

CONCLUSIONS

1. Rebound of the shale at the study site occurred during excavation, and was linear with respect to cut depth. The total amount of rebound at completion of the cut was approximately 0.7 feet.

2. Theoretical estimates of rebound using the Westergaard model for stress distribution in a nonisotropic elastic material compared in magnitude to the computed rebound using the finite element analysis. The best estimates of rebound were obtained from test data from the pressuremeter, consolidometer, and unconfined compressive strength tests. The computed values of rebound by these methods were 1.08, 0.72 and 0.54 feet, respectively.

3. Recorded inward side slope movement was small, less than one-half inch in most cases. Some lateral elastic rebound of the cut faces probably occurred concurrent with excavation, and prior to the installation of the extensometers. The extensometer data probably reflects the effects of high moisture content, rather than rebound from stress relief.

4. For this particular cut, the rebound has had little effect on the cut slopes and is not expected to affect future performance of the cut slope surface.

5. Attempts were made to calculate the elastic moduli on the basis of observed rebound. Results were inconclusive, due to problems in establishing boundary conditions for determinant analysis of an infinite elastic system.

RECOMMENDATIONS AND IMPLEMENTATION

While further field research in the analysis of rebound of cut slopes is an important subject to highway engineers, it is recommended that no further work be undertaken until more appropriate theoretical models and improved instrumentation are developed.

LITERATURE SURVEY OF
REBOUND MEASUREMENT AND ANALYSIS

1. Rebound of Shallow Excavations

Terzaghi[1] reported on two case studies of elastic heave which occurred during basement excavations in clay. The initial tangent modulus determined by unconfined compressive strength tests was used to predict rebound. Using a modulus of 100 tons per sq ft (1,380 psi), a heave of 5 in. was predicted at one site; with a heave of 3.5 in. observed. For the other building, a heave of 14 inches was predicted for a clay layer below the basement excavation, using an average modulus of elasticity of 60 tons per sq ft (835 psi). However, almost no heave was recorded in this strata. (Serota and Jennings were of the opinion that the lack of heave may have been due to the dewatering operation.) The method of calculating the expected vertical movement was not described.

Serota and Jennings[2] reported on the elastic rebound of shallow excavations up to 30 ft in depth. In one case, a backfilled-dewatered trench 10 ft deep was observed to rebound 3/16 in. as the water was allowed to rise. When the water table was lowered again, the trench settled 3/16 in. It was concluded that dewatering tends to compensate for elastic rebound due to excavation of soil.

The rebound of a clay strata about 84 ft thick located beneath the excavation for a large multi-story office building in London was measured[3]. This amounted to 0.5 in. at one excavation which corresponded to a pressure relief of 0.95 tons per sq ft. A net settlement of 0.075 in. was recorded after construction of the building. A modulus of elasticity of 1,200 tons/sq ft (16,600 psi) was estimated for the

formation; using the Steinbrener foundation-type formula expressed in terms of load relief, width of unloaded area, and an influence factor. The theoretical heave calculated using a modulus of elasticity determined from undrained triaxial tests was stated as being much too large.

The bottom heave of excavations in Leda clay for the Ottawa sewer plant was measured by Bozozuk[4]. He indicated that elastic settlement due to dewatering exceeded the heave due to removal of material for the primary settlement tanks, which were excavated to a depth of 12 ft. However, the elastic heave measured at the bottom of the 31.5 ft excavation for the digestion tanks was in the order of 0.5 in. This increased to about 1.0 in. due to swelling. Additional heave was attributed to pile driving at a later period. Using the same formula as employed by Serota and Jennings, moduli of elasticity of 822, 720, 591 kg/sq cm were calculated for the clay using Poisson's ratios of 0.3, 0.4 and 0.5 respectively. The maximum initial tangent modulus, determined by unconfined compressive strength tests on specimens trimmed from large undisturbed block samples, was given as 753 kg/sq cm (approximately 10,500 psi) and corresponded to the modulus calculated for Poisson's ratio of 0.4.

2. Rebound of Excavations for Dams

An extensive testing program was conducted by the Corps of Engineers to determine the properties of the Fort Union clay shales prior to the design and construction of the Garrison Dam, on the Missouri River at Riverdale, North Dakota[5,6].

This program included consolidation and rebound testing in a specially constructed high pressure consolidometer. Constant stress ratio triaxial tests were also conducted to determine a modulus of deformation (not defined in this report). The value of this modulus was given as 2,000 tons/sq ft (27,800 psi), and was used in estimating the elastic rebound. The calculated and measured elastic rebound was in the order of 0.8 to 1.0 ft for an excavation of approximately 180 ft in depth. Time dependent movements added another 0.7 to 1.0 ft to the measured rebound in two to three years after excavation. A finite depth of influence was assumed, with a maximum of approximately 350 ft. Vertical pressure changes were computed using the Boussinesq stress distribution. In general, the movements were reported to reflect the topography of the original ground.

In the program of investigation for the Oahe Dam, located in Central South Dakota on the Missouri River, Underwood reported that the static modulus of elasticity ranged from 20,000 to 140,000 psi[7]. The foundation material at the site is a typical Pierre shale. An in-place modulus of 100,000 psi was estimated on the basis of movement of an underground benchmark. The method of calculation was not given. Observation of this benchmark indicated that approximately 8 in. of rebound occurred during, or immediately after, excavation to a 200 ft depth. As the excavation approached final grade, an abrupt differential rebound (or rupture) occurred in the bottom along pre-existing fault lines. This movement was as much as 1.1 ft. During the following year shallow expansion of the top 10 ft below the bottom surface of the excavation ranged from 3 to 10 inches.

Arnold described the testing of sandstone and shales prior to excavation of the Delta Pumping Plant at Tracy, California. The static secant elastic modulus (5 to 22 kips/sq ft) of

approximately 50 samples averaged 70,000 psi, with a range of 4,000 to 140,000 psi[8]. Poisson's ratio was calculated on the basis of lateral strain measurements of core samples, and averaged 0.13 and 0.17 parallel and normal to the bedding planes, respectively. Laboratory sonic tests were conducted on the cores, and an average elastic modulus of 360,000 psi was found, although results were considered inconsistent. The elastic modulus was also estimated from field seismic tests (assuming Poisson's ratio = 0.4); and was found to be in the order of 730,000 psi.

The elastic rebound was predicted to be approximately 0.4 ft for an excavation of approximately 175 ft. Details for making this estimate were not given. It was later reported that the elastic rebound measured was slightly less than 0.3 ft[9].

A total of 0.7 ft of rebound accompanied the 115 ft excavation for the Dos Amigos Pumping Plant, San Luis, California[10]. The rebound benchmarks were installed at various depths, and it was ascertained that most of the movement (0.5 ft) occurred in the top 30 ft below final grade. This distance included 5.5 ft of alluvium, and about half of a 44 ft layer of underlying clay, which is described as a, "--highly plastic montmorillonitic soil". Rebound was estimated using one-dimensional consolidation theory, and the data from "stress-path" consolidation tests. The computed rebound of the top 50 ft of material remaining after excavation was 0.53 ft. The field measurements indicated about 0.6 ft of rebound occurring within the same depth. An important observation was that the rebound occurred much more rapidly (concurrently with excavation) than would be expected on the basis of consolidation theory.

An apparent "in-situ" modulus of elasticity of 150,000 psi was reported by Klohn for a dense glacial till deposit[11]. This investigation was made for the construction of a 100 ft

high combined earth and concrete dam. The Steinbrenner approximation method of computing settlement due to loads on the surface of an elastic layer was used to calculate the modulus. These results agreed fairly well with a modulus determined on the basis of plate bearing tests conducted in 50 ft deep test shafts. However, moduli computed from unconfined and triaxial compression tests were much too low. The rebound observed was in the order of 0.10 to 0.20 ft for the removal of 65 to 132 ft of material.

3. Effects of Stress History, Field and Laboratory Observations

Field observations by K. Langer of excessive swelling pressures about a tunnel in clay (Paris) were discussed by Terzaghi [12]. The pressures were greatly in excess of the existing overburden. Testing had indicated a migration of water toward the expansion zone about the tunnel, and a corresponding loss of water from the surrounding clay. This suggested that the tendency of the clay to expand around the tunnel created a difference in head between the two zones, thereby causing the flow of water. Stated otherwise, the swelling caused the flow of water, rather than the flow of water causing the swelling. Terzaghi concluded that this tendency to expand could not occur without the existence of excessive horizontal stress, presumably due to past overburden.

Saw cuts 3 inches wide and 7 ft deep were made in a clay shale during the field investigation for the previously discussed Garrison Dam [5]. These saw cuts closed in about 24 hours. The authors state, "This was attributed to yield caused by the release of tremendous lateral pressures that were induced by the overburden, which in the past ages was more than 1,500 ft higher than at present".

Underwood concluded that the sudden upward rupture of material in the bottom of the excavation for the Oahe Dam[7], as mentioned previously, was caused by the existence of high lateral compressive stresses. The shale was estimated to have been consolidated under an overburden load of 80 to 100 tons per sq ft sometime during its geological history. The overburden stress prior to excavation for the dam was in the order of 12 tons per sq ft.

During the investigation of a proposed dam site on the South Saskatchewan River in Western Canada, Peterson reported that the horizontal pressure in the preconsolidated clay-shale (the Bearpaw formation) was approximately 150 percent of the vertical[13,14]. This conclusion was based on observations over a two year period of a prestressed pressure test chamber with about 65 ft of overburden and shale above. The excavation of a 6-ft wide test drift intercepted a plane of movement between an underlying hard shale, and a softer shale. The drift was shored, but the softer shale moved into the space between bents so that the initial width decreased 11 to 21 inches. The width of the drift narrowed only 0.3 inches in the hard shale, and the monuments moved vertically only 0.3 inches. Most of these movements occurred within a few weeks.

An investigation of a failure of a 40 ft cut in over-consolidated London clay was described by Skempton[15]. He found that the capillary pressures within soil samples taken in the vicinity were approximately twice the vertical effective overburden pressure. He concluded that the coefficient of lateral earth pressure (K_o) was in the order of 2.0 to 2.5, caused by its prior overburden. His stability analysis of the failure also indicated high horizontal stresses.

Kjellman reported the testing of sands in an elaborate test apparatus which permitted the control of 3-dimensional stress-strain of a sample[16]. He indicated that the ratio of lateral pressure to axial pressure (in a one-dimensional compression test) varied from 0.5 to 1.5 on the rebound portion of the test curve at the lower stress levels. For triaxial tests conducted with no lateral strain, Bishop presents data for a variety of soils[17]. He states that the ratio of lateral stress to vertical stress approaches and may exceed unity in the terminal portion of the rebound test curve.

Brooker and Ireland (1965) used a high pressure consolidometer to conduct tests on remoulded cohesive soils[18]. The consolidometer chamber had an annular cavity which was lined with a steel membrane, and lateral strain during testing could be prevented by applying compensating hydraulic pressure in the annulus. To study the effects of over-consolidation, K_o was determined during the rebound portion of the test curves after loading and consolidation. It was concluded that, "For values of the over-consolidation ratio greater than about 20, the value of K_o appears to approach the coefficient of passive earth pressure and probably becomes equal to K_p".

Bjerrum (1967) presented a general theory to account for the often observed failure of slopes in stiff clays or clay shales at stresses estimated to be less than the effective shear strength of the materials[19]. Several of these failures are described. He concluded that the recoverable strain energy in a soil needs to be considered in stability analyses in these materials. Release of the strain energy is time dependent and a function of the strength of the diagenetic bonds which have been developed between the soil particle contact points. The energy is released almost immediately in clays with weak bonds. With strong bonds the release requires some further activity. This occurs as a result of weathering which gradually destroys the diagenetic bonds, releasing the locked-in strain

energy. This may in turn cause the progressive development of a sliding surface of failure; permitting a landslide to occur at some time after excavation.

In reference to Bjerrum's paper, Brooker discussed further his testing with the high pressure consolidometer[20]. He presents data to indicate that the area within the hysteresis loop could be considered as strain energy, and was proportional to the tendency to have a high K_o on rebound. The soils with the greater plasticity appeared to demonstrate this relationship best; as well as a more rapid and severe disintegration during slaking tests. (In the earlier report, Brooker concludes that the medium to low plasticity soils develop higher values of K_o than either the cohesive or highly plastic soils[18, p.11].)

Duncan and Dunlop employed the finite element method (plane strain) to investigate the theoretical effects of residual stress on the stability of an excavation in overconsolidated clay[21]. They concluded that the shearing stresses developed by an excavation in a soil with, "---high initial horizontal stress may vary between 171% and 224% of the values for the same configuration with low initial horizontal stress." Alternately, the analysis indicated that a higher safety factor (by the conventional equilibrium method) is required for excavation in heavily overconsolidated soils.

RESEARCH PROJECT

1. Proposal

In August 1964, the Geology Unit of the Foundation Section, Transportation Laboratory, introduced a proposal for research to investigate the rebound of materials in some of the deep cuts (up to 300 ft) now being routinely made in California highway construction. The amount, duration, and distribution of rebound was to be measured for possible influence on cut stability. Specifically an investigation was proposed of the rebound of a 260 ft cut to be made during construction of Interstate 5 north of Los Angeles. The project site between Castaic and Gorman is shown on Figure 1. This excavation would occur in the Ridge Route shale formation, a compacted shale of recent geological origin. A plan and cross-section of the cut is shown on Figure 2. The bottom of the cut is approximately 150 ft wide and the top is nearly 1,500 ft wide. There are 2:1 slopes between the bottom and the first bench, and 1-1/2:1 slopes from there to the top of the cut. There are four 30-ft benches on the westerly face, and five 30-ft benches on the easterly face.

The work plan included provisions for the installation of rebound monuments, prior to excavation, at elevations below final grade. A water level device, similar to a settlement platform, was also placed in a horizontal borehole for the purpose of measuring rebound. Extensometers were placed immediately after excavation with anchors to a depth of 50-ft behind the cut faces for the purpose of measuring their subsequent expansion or rebound. Provision was included for testing of core samples taken from boreholes to determine their physical and elastic properties. The analysis included the predicted rebound correlated with the actual.

2. Geology

The Ridge Route formation is a thick series of non-marine beds that overlay Modelo strata in the Ridge Basin, Figure 3. This is a northwestward trending structural basin between the San Gabriel and San Andreas fault zones in the transverse ranges of California. The beds are classed as latest upper Miocene or early Pliocene. The beds have been folded concordantly with the underlaying Modelo strata into a northwestward plunging ridge basin syncline. In the cut area they dip about 20° in a westerly direction.

Cores taken from the benchmark boring indicated for the most part a very hard uniform gray shale, with occasional laminates of sandy shale. Some fault material was found at a depth which would be near the bottom of the finished cut. Since this amount did not appear to be extensive, the cut was assumed to be underlayed by a uniform hard shale of undetermined depth for the purpose of rebound analysis. The boring profile is presented on Figure 4.

The excavation of the cut began in late 1965 and was virtually completed by February, 1967. Heavy ripping was required to break the shale loose, but upon exposure the material decomposed rapidly to a silty-clayey-sandy material of much lower strength. A small slide developed shortly after excavation at the south end of the westerly face in a zone of more weathered material, Photo 1. This was dressed back several times, as the condition became worse, until the slope appears as is shown in Photo 2, taken in March, 1970.

3. Movement During and After Excavation of the Cut

a. Subsurface Benchmarks

Prior to the start of excavation, two subsurface benchmarks were installed in the boring at about centerline Station 64+00. These benchmarks were anchored at a depth which would be just below the bottom of the completed cut. The uppermost of the benchmarks was extended to the surface by means of sections of steel rod, for which the original elevations of the joints and gage points were computed. As the rod was exposed, it was shortened section by section and the elevations of the gage points measured by survey. This provided a means of measuring the movements of the benchmark during excavation. See Photos 3 and 4.

The bottom benchmark was independent of the upper extended benchmark. The elevation of a mark on this lower unit was determined when installed and again when excavated. This provided a measurement of total rebound which was independent of the extended benchmark.

b. Water Level Device

A horizontal boring was made in which a manometer type water level device was placed. With this instrumentation the change in elevation of one end relative to the other should have been possible, thus providing another means of measuring the rebound. The water level device began giving erratic readings soon after its installation so that the resulting data are not considered meaningful.

c. Rebound of Subsurface Benchmarks

The data obtained from the extended benchmark is shown on Figure 5. The rebound of the benchmark is plotted arithmetically

against the nominal depth of excavation. A close linear relationship is demonstrated by this graph. The discontinuity in the trend line (drawn by visual estimate) is believed to be due to a surveying error in a transfer of reference benchmark. When adjusted, a total rebound of 0.7 ft is estimated. This rebound appeared to occur concurrently with excavation rather than over a period of time, thus indicating an elastic type rebound.

Following completion of the cut in January 1967, a surface monument was established in the median of the freeway to be used as a benchmark for future measurements of rebound of the cut floor. This monument was subsequently lost during construction operations.

d. Extensometers

As excavation progressed downward, extensometers were installed above most of the benches to measure the movement of the cut faces. These consisted of a long 3/16 in. rod attached to a rock bolt anchor placed to a depth of approximately 50 ft. The extensometer rod passed through a reference pipe anchored near the surface of the slope. Any differential movement was measured periodically with a dial indicator. See Photos 5 and 6.

A considerable variation in the movements of the outer cut faces after excavation has been indicated by the extensometer data. Plots of these data with respect to time are shown on Figures 6 through 14. Total movements and rates of movement are indicated on these figures. (The rate of movement is an overall estimate. The data during the period of more frequent readings indicate somewhat greater activity during the winter months.) Individual extensometer locations are shown on Figure 2A.

On the southern side of the western cut face, an expansion of approximately 0.8 in./yr was recorded with extensometer No. 10 (Figure 10) during the period October 1966 to March 1969. This instrument is located between the 2nd and 3rd benches from the bottom. A small slide developed adjacent to extensometer No. 10 shortly after it was installed, see Photo 1. This minor slide required early maintenance, which involved removal of a portion of the 3rd bench and grading of the disturbed portion of the cut face. The approximately constant rate of movement indicated by the data from extensometer No. 10 apparently reflected the internal strains which preceded a larger slide at the same location. This earth movement occurred between the reading periods of February 1969 and March 1970, and took out extensometers No. 9, 10 and 17. At that time, a total expansion of 1.88" within the outer 50 ft of the cut face was measured with extensometer No. 10. However, extensometers Numbers 9 and 17 (Figures 9 and 13) had shown little movement. The anchors of these two instruments may have been above the zone of most active movement, or the inner anchors may not have remained seated.

On the northern side of the western cut face, a somewhat similar pattern of movement is indicated by the data from extensometers Nos. 8, 11 and 16 (Figures 9, 11 and 14). Almost no movement has been measured with extensometers Nos. 8 and 11; but the data taken from No. 16 reflects an expansion of the cut face at the rate of approximately 0.8 in. per year. As noted on Figure 2-A, extensometer No. 16 is adjacent to a localized instability which became evident shortly after excavation of the cut face. At the time of the February 1970 reading, a total of approximately 2.45 in. of outward movement was indicated by No. 16. The inner anchor for extensometer No. 16 was placed at a depth of 38 ft rather than 50 ft due to an obstruction in the hole.

On the eastern cut face, not as much activity was evident. The extensometer which reflected the most movement was No. 3 (Figure 7). Data from this instrument indicates a total of about 1.65 in. of outward movement, which has been occurring at a rate of about 0.45 in. per year since October 1966. Extensometer No. 4 (Figure 6), which is adjacent to No. 3, has shown little movement since the first year, but has been out of commission since 1967 because of a loose outer anchor. The extensometers located just below the top of the easterly cut face, and above extensometer No. 3 (Nos. 1 and 2 as shown on Figure 6) have also shown little activity.

However, a total movement of 1.0 in. was measured at Extensometer No. 5 (Figure 8), which is located at about the same elevation as No. 3; but on the other side of the cut face (see Figure 2A). This movement has occurred at a rate of 0.4 in. per year during 1967; slowing to about 0.15 in. per year during the period 1968-69. Considering the data from extensometers Nos. 3 and 5, it is concluded that significant movement may have occurred at the top of the eastern cut face. Also, the active zone may have been deeper than the 50-ft depth of the interior anchors for extensometers No. 1 and 2, which could account for the lack of movement measured with them.

The total movements indicated by the remaining extensometers on the eastern cut face, located between the 1st and 4th benches, ranged from 0.10 in. to 0.71 in. Extensometer Nos. 6 and 7 (Figure 9), located between the third and fourth bench showed negligible movement. However, extensometers 12 and 13 (Figures 11 and 12) between the 2nd and 3rd bench which initially showed little movement, began to evidence an accelerated movement in late 1967. Since that time, movement of the cut face in the vicinity of these extensometers has continued at an approximately constant rate of 0.15 to 0.20 in.yr through the study period.

Relatively little activity was indicated by extensometer No. 14 (Figure 11) located between the 1st and 2nd bench on the eastern cut face as shown on Figure 2A. However, a steady expansion at the rate of approximately 0.06 in./yr has been observed by measurement of extensometer No. 15 (Figure 13), which was installed between the same two benches.

In summary, it is observed that the extensometers showing movement, tend to exhibit a constant rate of activity. Those showing the greatest movement are in the vicinity of slides or "pop-outs". Those showing the movements of next greatest magnitude tend to be toward the extremes of the cut faces. As seen on the eastern cut face, the rates of movements are greatest near the top of the cut, and diminish with depth toward the bottom of the cut.

There is one more observation which may be of importance. The possibility must be considered that the movements indicated by the extensometers only reflect the superficial weathering of the shale on the surface of the cut faces. However, this was discounted after consideration of the fact that the exposure to weathering was essentially uniform over the cut face. Consequently, if the movements were due solely to weathering after excavation; it would be expected that the movements measured with the extensometers would be more nearly uniform.

It is concluded that further study of movements of cut faces in sedimentary materials would be beneficial. A greater knowledge of the magnitude and rate of movement of these materials after excavation could provide a useful method of gaging the stability of these slopes. A two-position extensometer would also be useful in studying the expansion or movement phenomenon more closely.

4. Seismic and Borehole Strength Testing

a. Seismic Survey

A shallow seismic refraction survey was conducted in the vicinity of the cut prior to excavation. The results indicated three velocity zones. The uppermost of these had an average velocity of 2,250 fps, the middle 6,350 fps, and the lowest 7,475 fps. The break in the velocity profile between the 2,250 and 6,350 fps materials was estimated to be at a depth of approximately 33 ft. The 7,475 fps material was estimated to lie at a depth of 67 ft. The differences in velocities is believed to reflect the various stages of weathering of the shale.

A second series of seismic refraction lines were run in August 1967, seven months after completion of the excavation. This involved three lines along the 3rd bench from the bottom of the western cut face, Figure 2-A. This location was selected for seismic testing because of the proximity of the small slide on the south end of the bench. The results of this testing correlated well with the previous seismic data. Near the cut face the average velocity was 2,100 fps. Below this the velocity increased to an average 6,224 fps. The velocity break between those two zones occurred at a depth of 5 to 9 ft near the north end of the 3rd bench, but changed to a depth of 34 ft in the slide area on the south end.

The low velocities recorded in the second seismic series were within material for which velocities in the order of 6,000 to 7,000 fps were recorded in the earlier investigation. The 2,000 fps velocities recorded near the surface at the north end of the bench during the second seismic investigation were probably due to rapid weathering of the cut face, but may have also been caused by stress release due to unloading by the excavation.

b. Menard Pressuremeter

The Menard Pressuremeter was used to test extensometer borings Nos. 16 and 17 on the western cut face. The pressuremeter is a rubber-walled hydraulic cell device used for in-place testing of soils. Data on both stress and radial strain of the borehole during testing are obtained with this instrument. A schematic of the device is shown in Figure 15. A limited evaluation of the pressuremeter was reported by the California Division of Highways in 1968[22].

Widely differing strengths were obtained when testing the two borings. The yield stress in boring No. 16 was found to be 75 to 80 kg per sq cm, while in boring No. 17 it was found to be only 11 kg per sq cm (Figure 16). The apparent reason for this disparity in indicated strengths was that boring No. 16 was in sounder material, while boring No. 17 was in the weathered zone which later developed into a slide. However, as previously discussed, the extensometer in boring No. 16 continued to show a substantial rate of movement. The pressuremeter test data taken in this boring was used to calculate an in-place modulus for the shale.

5. Laboratory Testing of Shale Samples

a. Description of Testing Program

A laboratory testing program was conducted in conjunction with the field work. Samples of shale were subjected to stress-strain tests in the consolidometer and to unconfined compression tests. Void ratio, moisture content, X-ray-diffraction, differential thermal analysis (DTA) and grain size analysis tests were also performed.

The void ratio of shale samples taken from the boring for the subsurface rebound benchmark was approximately 0.40 near the surface, and decreased to about 0.25 at a depth of 75 ft. A less rapid decrease in void ratio with depth was indicated by sample data below this elevation, and a void ratio of 0.20 was estimated at a depth of 233 ft. In a fault zone located below the bottom of the cut (280 to 290 ft below the original ground profile) the void ratio varied from 0.30 to 0.49.

From the surface down, the moisture contents of the shale samples ranged from approximately 17 to 7 percent. The moisture contents of samples taken from the fault zone ranged from approximately 12 to 18 percent.

A mechanical analysis of the shale showed most of the material to be in the silt-sand size range, with the remaining portion in gravel or colloidal size. The DTA and X-ray analysis of samples taken at various locations indicated the shale to be composed of a variety of minerals as presented on Table 1. The analysis of the mineral composition did not appear to show any particular correlation with movement.

Core samples taken from the vertical boring for the rebound benchmark (centerline station 64+00) were shipped to the California Department of Water Resources Materials Testing Laboratory for triaxial tests to determine the modulus of elasticity and Poisson's ratio for the shale. Unfortunately, it was found that the samples contained hairline cracks and no positive results were obtained.

b. Consolidometer Stress-Strain Tests

Cores removed from the vertical benchmark boring were immediately placed in 2-in. diameter by 4-in. high brass sample tubes for

storage. These were then cut into one and two-inch high specimens without removal from the tubing in order to restrict their tendency to break along sedimentation planes. An initial series of tests were conducted in the consolidometer with these specimens still contained in their brass rings. The loadings in this set of tests ranged from 1/8 to 16 tons per sq ft (tsf), for a period of 15 to 25 minutes for each load increment. They were then unloaded or "rebounded" in similar increments. In some cases these cycles were repeated a number of times. Figure 17 represents the data acquired in the testing of a typical sample.

In these repetitive tests, a typical hysteresis loop, and a slight permanent set are noted; the latter decreasing with additional tests. As shown on Figure 17, a secant was drawn through the upper one-third of the rebound curves, and moduli were calculated. These moduli are discussed in greater detail in a subsequent section, "Modulus Calculations".

The consolidometer stress-strain data, when plotted arithmetically as in Figure 17, displayed a curvilinear relationship through the loading range. It was believed at the time that the cores might be slightly loose in the brass rings. Therefore, it would be possible that the samples could expand during testing; and it was believed that this could have contributed materially to the strains recorded. Consequently, it was decided to conduct tests in the consolidometer on samples which had been removed from their brass rings. These samples were not placed in the consolidometer sample holder, and were thus actually tested as unconfined specimens. Also, in this supplemental test series, the samples were left overnight under the maximum loading. The general performance of these samples under these test conditions is shown in Figure 18.

The first loading cycle plotted in Figure 18 was done as a control with the sample still retained in its brass ring, and not held under load overnight. The retaining ring was then removed, and the sample subjected to four additional cycles of loading and unloading. Of the total of 5 cycles, cycles 1, 3, and 5 are shown. The sample was only loaded to 2 tsf in cycle 2, which had little effect on the specimen. It is evident that in cycle 3, considerably more deformation of the sample occurred when loaded to 16 tsf in the unconfined state, than when confined and loaded to the same level of stress as in cycle 1.

Considerable permanent deformation or "set" of the sample was noted during loading cycle 3. The overnight creep of the sample under its maximum load contributed to the permanent deformation.

The rebound portions of cycles 3 and 5 are noticeably steeper than that of cycle 1 (Figure 18) at the higher stress levels. That is, the major portion of the strain recovery did not occur until the sample was almost completely unloaded. It was concluded that the samples had been effectively confined when originally tested in the consolidometer, and that the confinement tended to assist the strain recovery as the load was initially removed from the sample. This in effect decreased the apparent initial "stiffness" of the sample during unloading. This observation may be of some importance when interpreting stress-strain data for the purpose of acquiring an equivalent modulus of elasticity, such as for use in the finite element method of elastic analysis.

c. Unconfined Compression Tests

Tests were conducted to determine the rupture strength of unconfined samples of the shale. These specimens had similar dimensions as those tested in the consolidometer. Strain measurements were taken, and the results of testing three specimens are shown in Figure 19. In general, a linear

relationship was exhibited between stress and strain. Sample A was loaded at two rates, 250 and 1,000 lbs per minute, and a difference was noted. As would be expected, the specimen exhibited a greater stiffness, or resistance to deformation, at the higher rate of loading. This factor would have to be considered when interpreting stress-strain data from this type of test. Samples B and C were trimmed from the same core, but sample B had been previously tested in the consolidometer.

Two linear approximations of the test data are shown on Figure 19, one for sample C, and one for samples A and B combined. A discussion of the equivalent elastic moduli of these curves is given in the following section.

6. Modulus Calculations

Based on the various types of tests performed for this research, several values of elastic modulus have been calculated. The theoretical equations, and the values calculated, are summarized in the following paragraphs.

a. E_p, Pressuremeter Modulus

The elastic modulus as determined from pressuremeter data is calculated from the basic equation:

$$E_p = (1 + \mu) \frac{r\Delta P}{\Delta r} \qquad (1)$$

Where; Δp = the change in hydraulic pressure, r = the initial (nominal) radius of the borehole, Δr = change in radius of the borehole, μ = Poisson's ratio. The equation is derived from the equation for a thick walled elastic cylinder subjected to differential pressure. Change in radius (Δr) is estimated from the volume of fluid added (Δv) in the proportional range of stress versus strain from the field test data, Figure 16. The complete development of this equation is given in reference [22], and the resulting form is:

$$E_p^1 = (1 + \mu)\ 2\ V_o \frac{\Delta P}{\Delta V} \qquad (2)$$

In this equation, V_o is the calculated initial volume of the test probe when expanded to the nominal diameter of the borehole.

Two pressuremeter tests were conducted in extensometer hole #16. The modulus calculated for the test at a depth of 22 ft was $E_p = (1+\mu)$ (42,500 psi), Figure 16-B. A similar test of 38 ft had a modulus $E_p = (1+\mu)$ (90,000 psi). Assuming that Poisson's ratio (μ) is equal to 0.4, these become approximately 60,000

---

[1] In reference [22] the notation "E_p" is used to denote the apparent modulus based on field stress-strain data, without the form $(1+\mu)$.

and 125,000 psi respectively. It is noted that these moduli are taken in compression rather than rebound, as are the moduli determined from the high-stress unconfined compression tests conducted on shale samples in the laboratory.

b. E_c Consolidometer Modulus

The consolidometer moduli were calculated from the stress-strain tests as shown on Figures 17 and 18. The moduli for the unconfined specimens (Figure 18, cycles 3 and 5) were directly calculated on the basis of a secant arbitrarily drawn through the upper 1/3 of the rebound curves:

$$E_c = \frac{\Delta\sigma}{\Delta\varepsilon} \qquad (3)$$

In this equation, $\Delta\varepsilon$ is the change in strain in the direction of the change in principal stress, $\Delta\sigma$. The moduli for the confined consolidometer tests (Figures 17 and 18, cycle 1) were also calculated using equation 3.

Theoretically a correction $f(\mu)$ based on Poisson's ratio should be required when calculating moduli from confined consolidometer data. Assuming no lateral strain, this takes the form:

$$E_c = f(\mu) \quad \frac{\Delta\sigma}{\Delta\varepsilon}$$
$$E_c = \left(1 - \frac{2\mu^2}{1-\mu}\right) \frac{\Delta\sigma}{\Delta\varepsilon} \qquad (4)$$

However, as was noted, the rebound portion of the unconfined consolidometer curves is quite noticeably steeper than that of the confined specimens. As a result, the indicated arbitrary secant moduli calculated on the basis of the unconfined tests are also higher. Nominally, this would indicate that the unconfined specimens exhibit a greater stiffness than the confined. The use of equation 4 would increase the disparity.

Actually the differences observed are caused by the semiplastic characteristics of the material. In the unconfined test, such materials will strain in compression considerably more than indicated by the simple elastic equation 3. This is caused by time dependent plastic flow. Similarly, in rebound, the semi-plastic material will recover less strain in an unconfined test than when confined. The observed behavior of the semi-plastic material in rebound is therefore contrary to the trend indicated by the elastic equations 3 and 4. Consequently, for the purpose of this discussion, the confined consolidometer moduli were calculated using equation 3. This is equivalent to assuming Poisson's ratio (μ) to be zero in equation 4.

The consolidometer moduli are summarized as follows:

Cycle	Restraint	Stress (psi)	Mean Stress (psi)	E (psi)
1	yes	53 - 86	69	25,000
3	yes	75 - 111	93	25,000
5	yes	153 - 223	188	40,000
1	yes	153 - 223	188	50,000
3	no	153 - 223	188	60,000
5	no	292 - 446	369	75,000

These estimated values of the moduli of elasticity as determined by the various consolidometer tests are plotted versus their peak stress in Figure 20. The moduli obtained from the pressuremeter tests in the field and the high-stress unconfined compression tests are also shown on this figure. In general, an approximately linear increase in moduli with peak stress level appears to be indicated by the consolidometer data.

c. E_h Unconfined High-Stress Compression Modulus

Two moduli were calculated from the trend lines for the unconfined compression test data, as were shown in Figure 19. It is seen that these moduli (170,000, 290,000 psi) are substantially higher than were the consolidometer moduli. This conforms to the general trend for the shale modulus to increase as a function of stress level. However, the data for the unconfined high stress moduli are taken in compression rather than rebound, as well as by a strain rather than stress controlled test. As a result, there is room for question as to the relationship of these moduli with those previously determined from the consolidometer data.

The two unconfined high stress moduli are plotted versus their failure stress on Figure 20. A trend line is drawn through these data, assuming a zero intercept of moduli and stress, and a linear increase in the compression moduli with maximum stress. The assumption of a linear relationship between stress level and moduli seems to be confirmed by prior data published by Zisman[23], Tables 1 and 2, showing the variation in moduli obtained for two granite specimens at various mean stress levels. If these sets of data are plotted, even though the granite is a much stronger rock than the shale, a linear increase in moduli versus mean stress is evident. This is especially true for the second specimen[23, Table 2] which was tested to higher mean stress levels.

In Figure 20 it is apparent that the moduli calculated on the basis of the unconfined compression tests are much higher than would be expected on the basis of a projection of the consolidometer moduli data. This is presumably due to the fact that these tests are strain rather than stress controlled, the accelerated rate of loading of the samples, and the much higher stress levels. The moduli calculated on the basis of the pressuremeter test data appear to fall somewhere between the consolidometer and unconfined high stress moduli.

d. E_s Seismic Velocity Modulus

A modulus of elasticity may be estimated on the basis of the seismic velocity:

$$E_s = f(\mu) \frac{V^2 \gamma}{g} \qquad (5)$$

Equation 5 is obtained from the 3 dimensional compression wave equation, where V is velocity in fps, γ is the unit weight of material in lbs per cu ft, and g is the acceleration of gravity (fps). The function of Poisson's ratio (μ) is:

$$f(\mu) = \frac{(1 + \mu)(1 - 2\mu)}{(1 - \mu)} \qquad (6)$$

The following tabulation illustrates that $f(\mu)$ varies between 1.0 and 0.0 as (μ) increases from 0.0 to 0.5. The $f(\mu)$ is extremely sensitive to small variations in the value of (μ) greater than 0.3. Assuming that the seismic velocity of 7,475 fps from the preliminary survey is representative of the material at depth, the corresponding seismic moduli are shown:

μ	$f(\mu)$	E_s (psi)
0.0	1.000	1,690,000
0.1	0.978	1,650,000
0.2	0.900	1,520,000
0.3	0.743	1,260,000
0.35	0.623	1,050,000
0.40	0.467	788,000
0.45	0.264	445,000
0.50	0.000	0

If a value of Poisson's ratio of 0.3 is assumed, a seismic modulus (E_s) of 1,260,000 psi is obtained. This dynamic in-place modulus greatly exceeds those obtained by either static laboratory or field testing. A similar observation has been made by other investigators [24, p. 107].

7. Rebound Analysis by the Finite Element Method

For the purposes of calculating the theoretical rebound of the excavation, the plane-stress program written by Wilson[25] was employed, with the elastic constants modified for the plane-strain condition. The material was assumed to be homogeneous, isotropic, and linearly elastic. A modulus of elasticity "E" of 150,000 was arbitrarily assumed. The equivalent modulus for the field materials could then be estimated by comparing the calculated and measured rebound. A value for Poisson's ratio of 0.4 was assumed.

The approximate original ground profile, and the excavation cross-section, are shown on Figure 21 by solid lines. The outline of the configuration assumed for the analysis is represented by dashed lines. In this analysis, the cross-sections of the excavation were assumed to be uniform along its length, which permitted the problem to be treated as a two-dimensional plane-strain elasticity problem.

In order to make the problem determinate, it was necessary to assume finite boundary conditions which have a significant effect on the results. Since the assumption of perfect elasticity implies infinite boundaries, two arbitrary sets of boundary conditions were assumed as shown on Figure 22. The magnitude of rebound as calculated for the two conditions were then compared. This allowed extrapolation for the case of infinite boundaries and negligible change in stress. The lateral boundaries were assumed to be free to move vertically, and fixed in the horizontal direction. The bottom or horizontal boundary was considered fixed in both directions. For simplicity, the depth of excavation was considered to be 300 ft.

The effect of the excavation on the remaining material was simulated by applying loads which cause a stress-free condition on the face of

the cut. This was achieved by estimating the vertical and horizontal stresses existing along the cut surface due to the gravity loads prior to excavation. The lateral stresses were calculated assuming no lateral strain. The loads on each cut surface nodal point were then calculated by summing the stresses, and applying the negative of those loads. The unit weight of the material was assumed to be uniformly 140 pcf.

It has been demonstrated that it is necessary to analyze the stresses and strains created within embankments due to gravity loading by assuming incremental construction[26]. However, it has been generally concluded that in the case of excavations, the effect on the remaining material is satisfactorily approximated by assuming the material to be removed in one increment[21,27,28]. This procedure was followed in this study.

The rebound estimated at the bottom of the excavation for the smaller boundary conditions was 0.8 ft and for the larger boundary, 1.3 ft. From this information, it was determined that the rebound in the case of infinite boundaries would be in the order of 1.7 ft for the moduli of E = 150,000 psi and μ = 0.4.

8. Rebound Analysis by Westergaard, Boussinesq Stress Distributions - Incremental Approximation

The elastic rebound of an excavation may be estimated using the Westergaard or Boussinesq stress distributions. These are readily available for the case of an infinitely long load or foundation of some finite width. They are given in the form of influence curves of percent of vertical stress (at the surface), versus depth, as a function of width of load.

The Boussinesq stress distribution[29, p.251] assumes a perfectly elastic, homogeneous, isotropic material, and the vertical stress is independent of Poisson's ratio. The assumptions made in the Boussinesq solution are compatible with those made in the finite element method of analysis. Rebound may be estimated by an iterative procedure based on the general stress strain expression:

$$\varepsilon_1 = \frac{1}{E} [\sigma_1 - \mu(\sigma_2 + \sigma_3)] \qquad (7)$$

Where σ_1 = Change in vertical stress
σ_2;σ_3 = Changes in normal stress
E = Young's modulus of elasticity
μ = Poisson's ratio
ε_1 = Strain in the direction of change in vertical stress

It is noted that Poisson's ratio is required. Also, σ_2 and σ_3 are indeterminate in the practical case, being a function of σ_1, μ, and the degree of lateral and vertical strain permitted. However, if $\mu = 0$, equation (7) becomes:

$$\varepsilon_1 = \frac{\sigma_1}{E}$$

and the maximum strain would be obtained.

The effect of Poisson's ratio can be estimated as follows: If a condition of no lateral strain could be assumed

$$\sigma_2 = \sigma_3 = \frac{\mu}{1-\mu} \sigma_1 \qquad (8)$$

By substitution, equation (7) becomes:

$$\varepsilon_1 = \frac{\sigma_1}{E} (1 - \frac{2\mu^2}{1-\mu}) \qquad (9)$$

and the strain at a point would be reduced roughly 50 percent if μ were equal to 0.4, and about 25 percent if $\mu = 0.3$. In the actual case, lateral strain is significant, which would limit the effect of Poisson's ratio to values less than indicated by equation (9).

The Westergaard solution[30] is obtained by assuming the material to be homogeneous and elastic. It is further assumed that the soil is reinforced with closely spaced horizontal flexible but unstretchable sheets. Thus, lateral strain is prevented, and the effect of a nonisotropic or layered soil is approximated. Vertical stress based on the Westergaard formula is dependent on Poisson's ratio; however the graphs available for the Westergaard vertical stress distribution are based on the simplifying assumption that $\mu = 0$. This results in a shallower stress distribution than the Boussinesq solution; the stress at centerline from Westergaard being approximately 2/3 of the Boussinesq. For a point load at centerline, and $\mu = 0.25$, the vertical stress from the Westergaard formula is equal to that of the Boussinesq. For higher values of μ, the Westergaard vertical stress coefficients exceed that of the Boussinesq. The principal justification for the use of the Westergaard stress distribution with $\mu = 0$ has been that settlement predictions using it in conjunction with consolidometer data have generally more closely approximated field measurements than those with Boussinesq.

Rebound of the Ridge Route excavation was estimated using both the Boussinesq and Westergaard stress distributions for a long continuous load. Since the depth of influence is dependent on the width of loading, the material was considered to be removed in 60 ft layers or increments. These were then treated as individual loads, and the mean width of each was used to determine the stress influence factors for that layer. This first model is illustrated in Figure 23. The distances between the selected stress contours were then estimated.

By summing the products of these distances times the average stresses between the contours selected, the total effect of the removal of the particular soil layer was estimated. This procedure was repeated for the remaining layers. An example calculation for one of the layers is as follows.

Sample Calculation for the Effect of Removal of Layer Number 4 - Westergaard Stress Distribution

Layer number	4
Layer thickness =	60 ft
Unit wt of soil =	140 pcf

Stress change at bottom of layer caused by its removal:

$\frac{P}{A}$ = 4.2 tons sq ft (tsf)

Shown below is this calculation in tabular form. The incremental thickness (L) is the distance between the selected influence lines. The average stress factor (w) for each increment is assumed to be the arithmetic mean of the stress factors bounding that increment at the centerline of the excavation. The average incremental stress is equal to the average stress factor (w) times the change in stress from the layer removed ($w \frac{P}{A}$).

Note that the thickness of increment #1 (*) is determined from bottom of cut, (layer 5) rather than from the bottom of layer 4.

When $\frac{P}{A}$ = 4.2 tsf

Increment	Incremental Thickness (L) ft	Average Westergaard Stress Factor (w)	Average Increment Stress ($w\frac{P}{A}$) tons per sq ft	($w \frac{P}{A}$).L tons per ft
1	50*	0.85*	3.6	180
2	165	0.7	2.9	479
	247	0.5	2.1	519
	688	0.3	1.2	826
	1238	0.15	0.6	743
			Total =	2747

Rebound for layer #4 = $\frac{2747 \text{ lbs/ft}}{E}$

Adding this sum to that found for the other layers, and dividing by "E" = 150,000 psi (as used in the finite element analysis), a total rebound of 1.75 ft was computed using $\mu = 0$.

A similar procedure was followed with the Boussinesq stress distribution with $\mu = 0$, and the rebound was calculated to be 2.5 ft.

Rebound was also estimated with the Westergaard stress distribution applied to a second model. In this model, the soil was considered to be removed all at once. The effective width of the second model was simply assumed to be the average of the top and bottom widths of the cut (775 ft).

The rebound calculated on the basis of the single increment approximation was 2.0 ft.

9. Comparison of Finite Element and Approximate Analyses

The results of the various rebound analyses is summarized as follows:

Method of Stress Analysis	Rebound (ft) $\mu = 0.0$	$\mu = 0.4$
Finite element	-	1.7
Westergaard (5 increments)	1.7	-
Westergaard (1 increment)	2.0	-
Boussinesq	2.5	-

A review of the foregoing table illustrates that the Boussinesq stress distribution with $\mu = 0$ yields the maximum value of rebound. If it is assumed that the results of the Boussinesq and finite element method are compatible, it is concluded that the range of 2.5 to 1.7 ft of rebound, represents the effect of Poisson's ratio as it varies from 0.0 to 0.4. Thus, the effect of intermediate values of Poisson's ratio can be estimated.

The Westergaard (5 increment) analysis agrees in magnitude with the finite element rebound for $\mu = 0.4$. Also the rebound by the Westergaard (5 increment) is almost exactly two-thirds that of the Boussinesq, which is the same ratio as the respective stresses at centerline caused by a point load at the surface.

A rebound of 0.7 ft was observed at the field site. By direct proportion, after adjusting for the difference between the actual depth of excavation (260 ft) and that assumed in the theoretical analyses (300 ft), it was estimated that the equivalent moduli were:

	"E" psi	
Method of Analysis	$\mu = 0.0$	$\mu = 0.4$
Finite element	-	315,000
Boussinesq (5-layer)	465,000	-
Westergaard (5-layer)	315,000	-
Westergaard (1-layer)	370,000	-

At this point the following observations can be made concerning the correlation of the apparent field moduli and the moduli determined by the various field and laboratory tests. The following is a tabulation of the average or representative moduli.

Representative Moduli

Test	"E_1" psi	"μ"
Consolidometer (rebound)	50,000	-
Pressuremeter (compression)	93,000	0.4
High stress (compression)	230,000	-
Seismic (compression)	778,000	0.4

If it is presumed that the field modulus of 315,000 ($\mu = 0.4$) indicated by the finite element analysis is correct, it is apparent that the best agreement is given by the unconfined compression modulus, which is about 75 percent of the field modulus. The consolidometer and pressurementer moduli are also considerably lower than the indicated field modulus and the seismic modulus is about twice that of the field.

In review, it was tentative concluded that the stress distribution implied by the assumption of a perfectly elastic material is in error. In actuality, the zone of material affected by the excavation is probably much less than that implied by elastic theory. As a consequence, the lower moduli as determined by the static field and laboratory tests are probably more nearly correct than it appears on first inspection.

REFERENCES

1. Terzaghi, Karl, Peck, R. B., "Soil Mechanics in Engineering Practice", John Wiley and Sons, New York, New York, pp 450-453, 1948.

2. Serota, S., Jennings, R. A. J., "Elastic Heave in the Bottom of Excavations", Geotechnique, Vol. IX, No. 2., June, 1959.

3. Terzaghi, K., "Theoretical Soil Mechanics", John Wiley and Sons, New York, New York, pp 423-427, 1943.

4. Bozozuk, M., "The Modulus of Elasticity of Leda Clay from Field Measurements", Canadian Geotechnical Journal, Vol. I, No. 1, September 1963.

5. Smith, Carneal K., Redlinger, J. F., "Soil Properties of Fort Union Clay Shale", 3rd International Conference on Soil Mechanics and Foundation Engineering, Proceedings, Vol. I, pp 62-66, 1953.

6. Lane, K. S., Occhipinti, S. J., "Rebound Gages Check Movement Analysis at Garrison Dam", 3rd International Conference on Soil Mechanics and Foundation Engineering, Proceedings, Vol. I, pp 402-405, 1953.

7. Underwood, L. B., Thornfinnson, S. T., Black, W. T., "Rebound in Design of Oahe Dam Hydraulic Structures", Journal SMFD-ASCE, pp 64-86, March, 1964.

8. Arnold, A. B., "Results of the Foundation Investigation and Rock Testing for the Delta Pumping Plant, Tracy, California", Presentation - 6th Annual Meeting, Association of Engineering Geologists, San Francisco, October 25-27, 1963.

9. O'Neill, A. L., Scott, J. F., "Influence of Engineering Geology on Design and Construction of the Delta Pumping Plant Site - California State Water Project", Presentation - 1965 Annual Meeting Geological Society of America, Kansas City, Missouri, November 4, 1965.

10. Bara, J. P., Hill, R. R., "Foundation Rebound at Dos Amigos Pumping Plant", Journal SMFD-ASCE, pp 153-168, September, 1967.

11. Klohn, Earle J., "The Elastic Properties of Dense Glacial Till Deposit", Canadian Geotechnical Journal, Vol. II, No. 2, May, 1965.

12. Langer, K., "Field Observations (Discussed by K. Terzaghi)", Proceedings, Foundation Engineering, Vol. 3, pp 152-155, 1936.

13. Peterson, R., "Studies of Bearpaw Shale at a Damsite in Saskatchewan", Journal ASCE-SMFD, Vol. 80, Separate No. 476, New York, August, 1954.

14. Peterson, R., "Rebound in the Bearpaw Shale Western Canada", Bulletin Geological Society of America, Vol. 69, No. 9, pp 1113-1124, September 1958.

15. Skempton, A. W., "Horizontal Stresses in an Over-Consolidated Eocene Clay", Proceedings, 5th International Conference on Soil Mechanics and Foundation, Engineering Vol. I, pp 351-357, 1961.

16. Kjellman, W., "Report on an Apparatus for Consummate Investigation of Soils", Proceedings of the International Conference of Soil Mechanics and Foundation, Engineering Vol. II, pp 16-20, 1936.

17. Bishop, A. W., Henkel, D. J., "The Measurement of Soil Properties in the Triaxial Test", Edward Arnold Ltd., London, England, pp 140-144, 1957.

18. Brooker, E. W., Ireland, H. O., "Earth Pressures at Rest Related to Stress History", Canadian Geotechnical Journal Vol. II, No. 1, pp 1-15, February 1965. (Discussion by M. J. Horslev, pp 337-338, November, 1965.)

19. Bjerrum, Lauritas, "Progressive Failure in Slopes of Over-Consolidated Plastic Clay and Clay Shales", Journal SMFD-ASCE, September, 1967, Part 1, pp 3-49.

20. Brooker, E. W., "Strain Energy and Behavior of Overconsolidated Soils", Canadian Geotechnical Journal, Vol. IV No. 3, pp 326-333, September, 1967.

21. Duncan, J., Dunlop, P., "Slopes in Stiff-Fissured Clays and Shales", (Short Course Notes) Recent Advances in Soil Mechanics, June 10-14, 1968, University of California Extension, Los Angeles.

22. Smith, R. E., Smith, T. W., "Embankment Testing with the Menard Pressuremeter", M&R No. 632509-2, California Department of Public Works, Division of Highways, Sacramento, May, 1968.

23. Zisman, W. A., "Young's Modulus and Poisson's Ratio with Reference to Geophysical Applications", Proceedings National Academy of Science, 19, No. 7, 1933.

24. Mayer, Armand, "Recent Work in Rock Mechanics", (Third Ranking Lecture) Geotechnique, Vol. XIII, No. 2, London, England, June 1963.

25. Wilson, E. L., "Finite Element Analysis of Two-Dimensional Structures", PhD Thesis, University of California, 1963.

26. Clough, R. W., Woodward, R. J., "Analysis of Embankment Stresses and Deformations", Journal SMFD-ASCE, pp 529-549, July, 1967.

27. Brown, C. B., King, I. P., "Automatic Embankment Analysis: Equilibrium and Instability Conditions", Geotechnique, Vol. 16, No. 3, pp 209-219, 1966.

28. Goodman, L. E., Brown, C. B., "Dead Load Stresses and the Instability of Slopes", Journal SMFD-ASCE, pp 103-134, May, 1963.

29. Taylor, D. W., "Fundamentals of Soil Mechanics", John Wiley and Sons, New York, New York, 1948.

30. Westergaard, H. M., "A Problem of Elasticity Suggested by a Problem in Soil Mechanics: Soft Materials Reinforced by Numerous Strong Horizontal Sheets", The Stephen Timoshenko 60th Anniversary Volume, pp 268-277, MacMillan Company, 1938.

TABLE 1

ESTIMATE OF SOIL MINERALOGY IN PERCENT
BY
X-RAY DIFFRACTION AND DIFFERENTIAL THERMAL ANALYSIS

	SAMPLE LOCATION	AMPHIBOLE	FELDSPAR	QUARTZ	PYRITE (SULFIDE)	GYPSUM	CALCITE	DOLOMITE	ANALCITE	MICA	ILLITE	CHLORITE	MONTMORILLONITE	MIXED LAYER CLAY (EXPANSIVE)	IRON OXIDE	ORGANIC	OTHER
EASTERN FACE	Grade 1st Bench	<5	10	10-15		5	5	5	10-15	15-20		<5		10	<5	<5	5
	2nd, 3rd Bench		10	10-15	<5	5	5-10	10-15	10		10	5	5-10	5-10	<5	<5	<5
	4th,5th Bench		5-10	10-15	<5	5	5-10	10-15	10		10-15	<5		15	<5	<5	5
WESTERN FACE	Grade	5	5-10	10-15	5-10	5-10	5		15-20		10-15	5	5		<5	<5	5
	1st Bench		15-20	10-15	5	<5	5	5-10	10		10-15	<5		5-10	<5	5	5
	2nd,3rd, Bench	<5	5-10	10-15	5-10		10	5-10	15-20		10	<5	5		<5		5

Figure 1

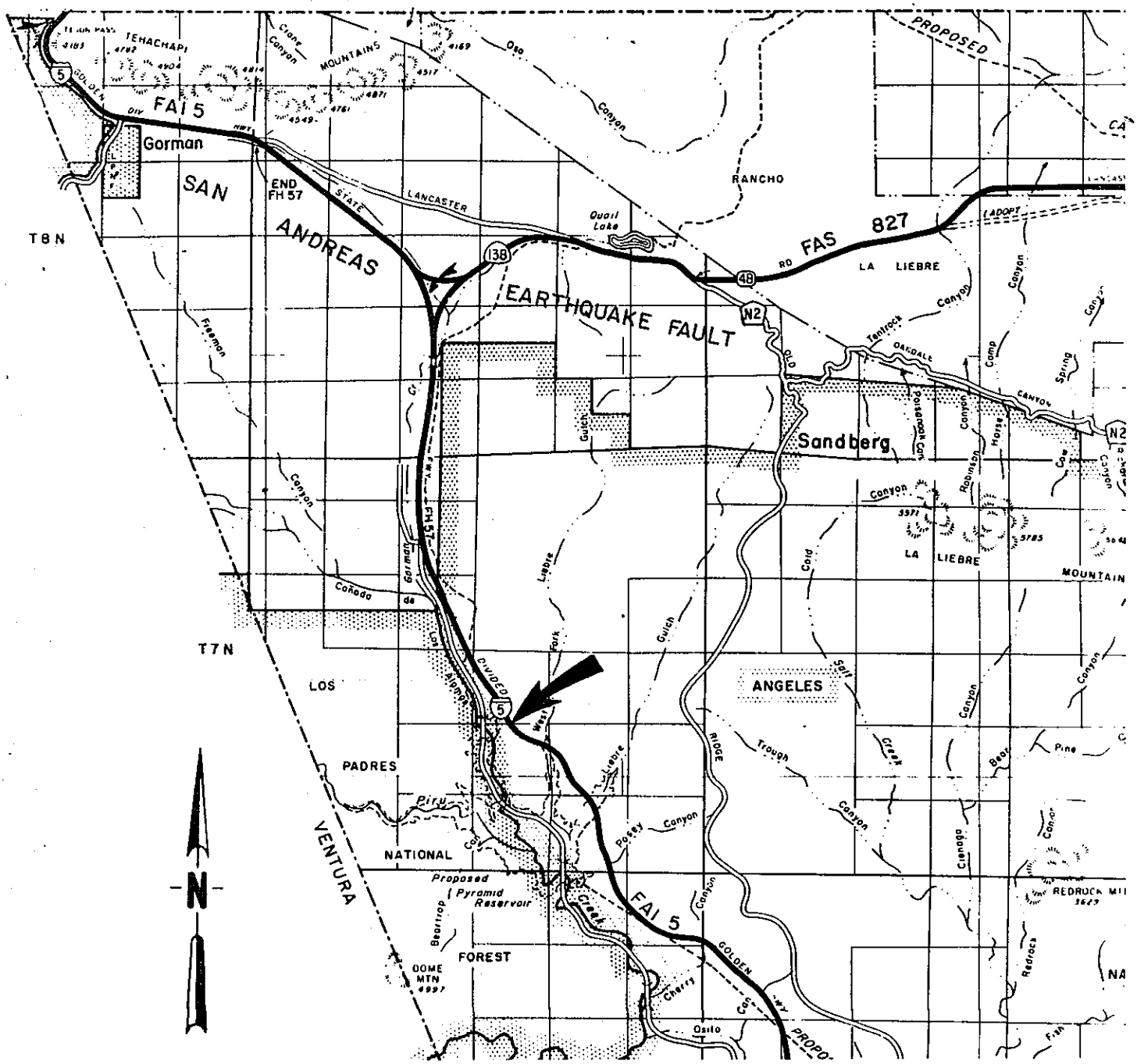

LOCATION MAP

Figure 2

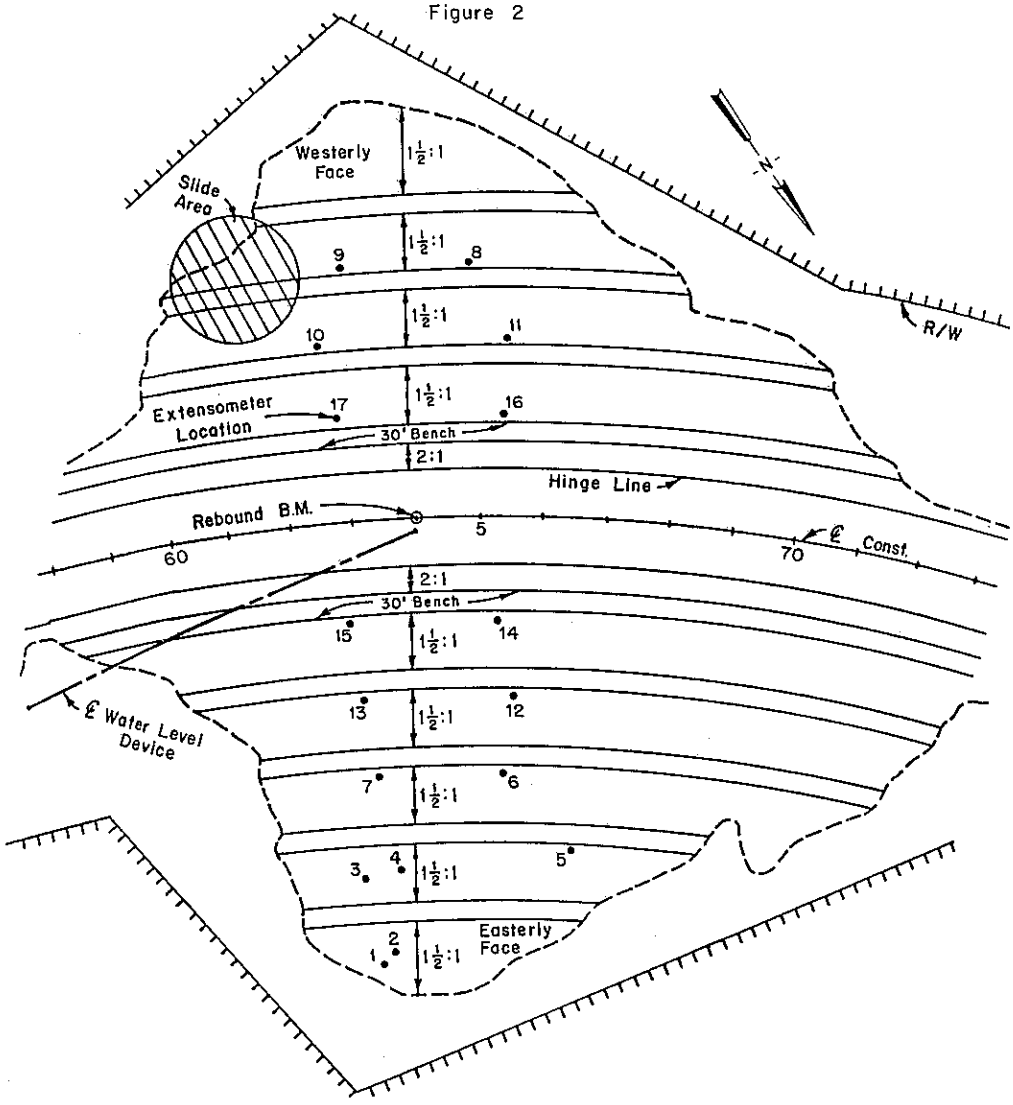

PLAN VIEW OF EXCAVATION

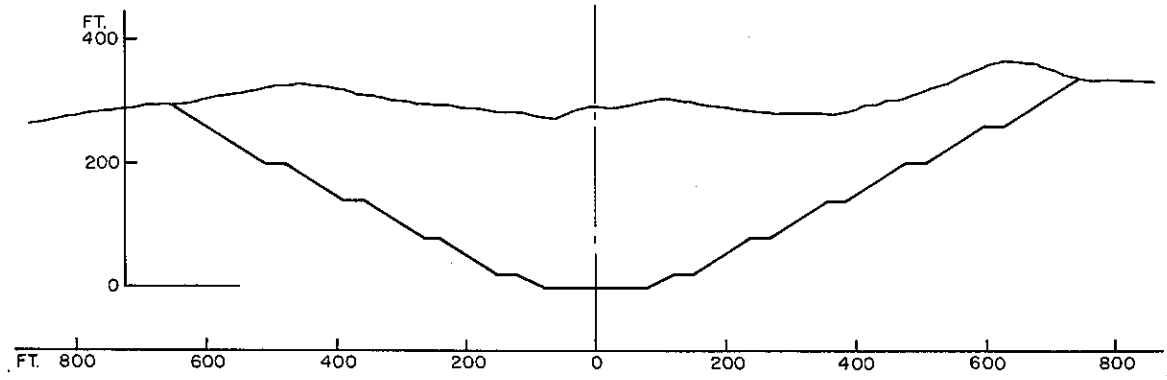

APPROXIMATE CROSS SECTION

Figure 3

STRUCTURAL SECTION THROUGH RIDGE BASIN

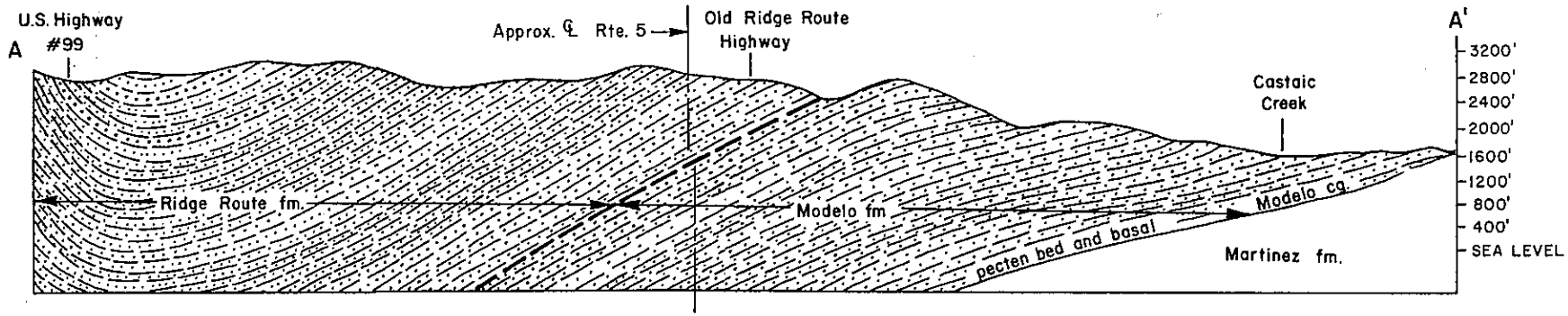

Figure 4

BORING PROFILE

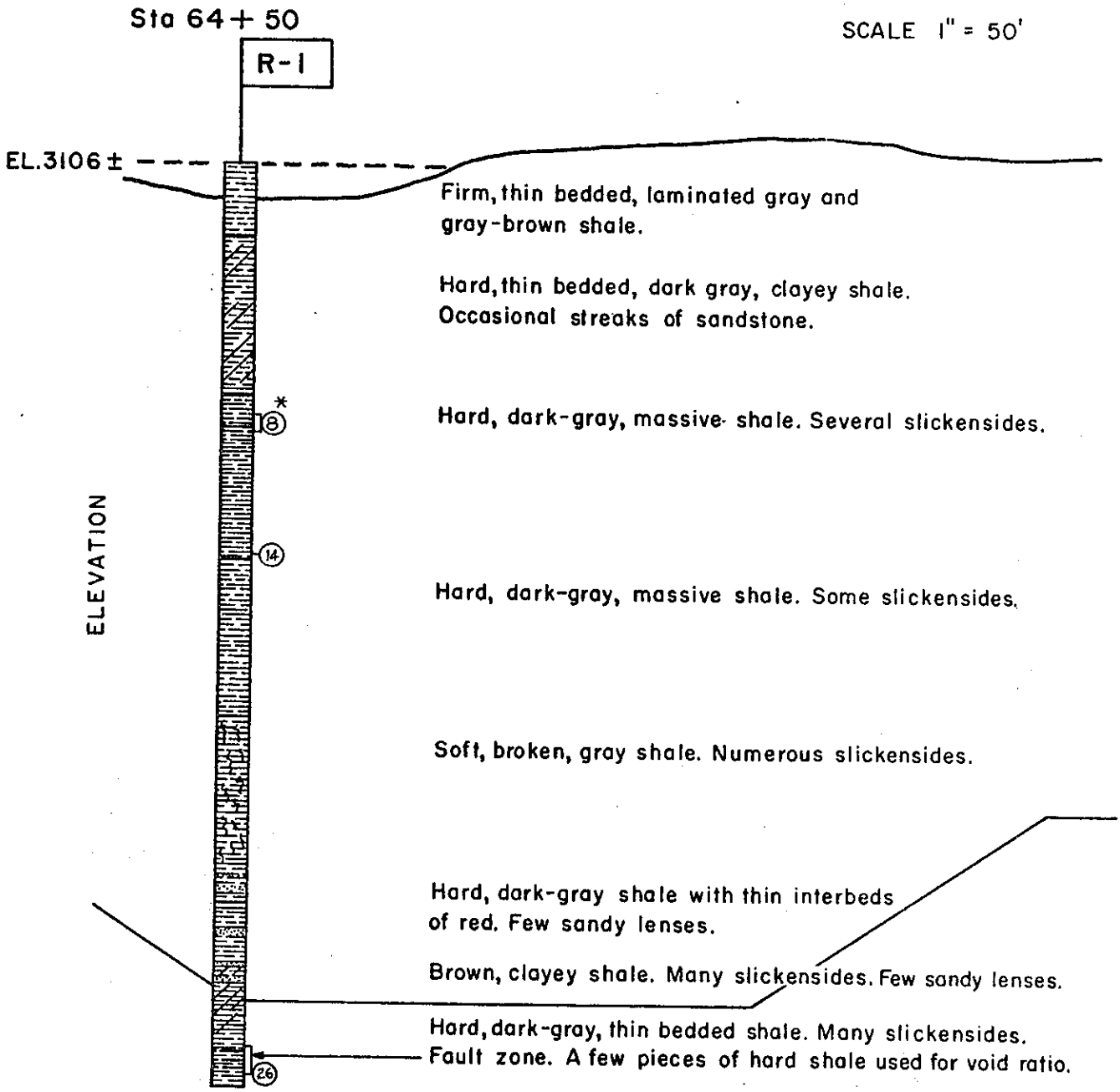

* Test Sample Location

Figure 5

BENCHMARK AT ℄ STA. 64+00
REBOUND VS CUT DEPTH

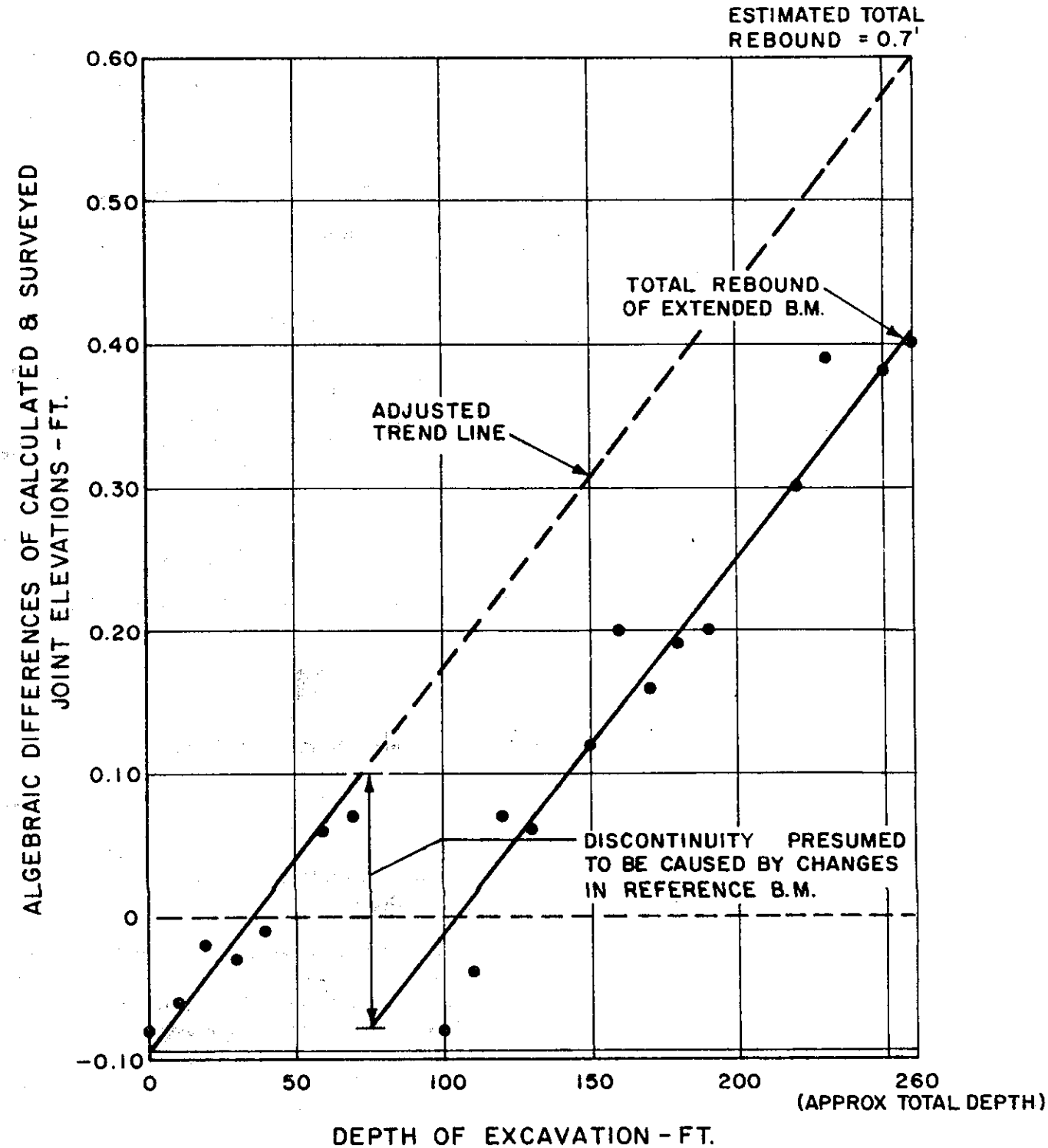

Figure 6

EXTENSOMETER MOVEMENT VS TIME

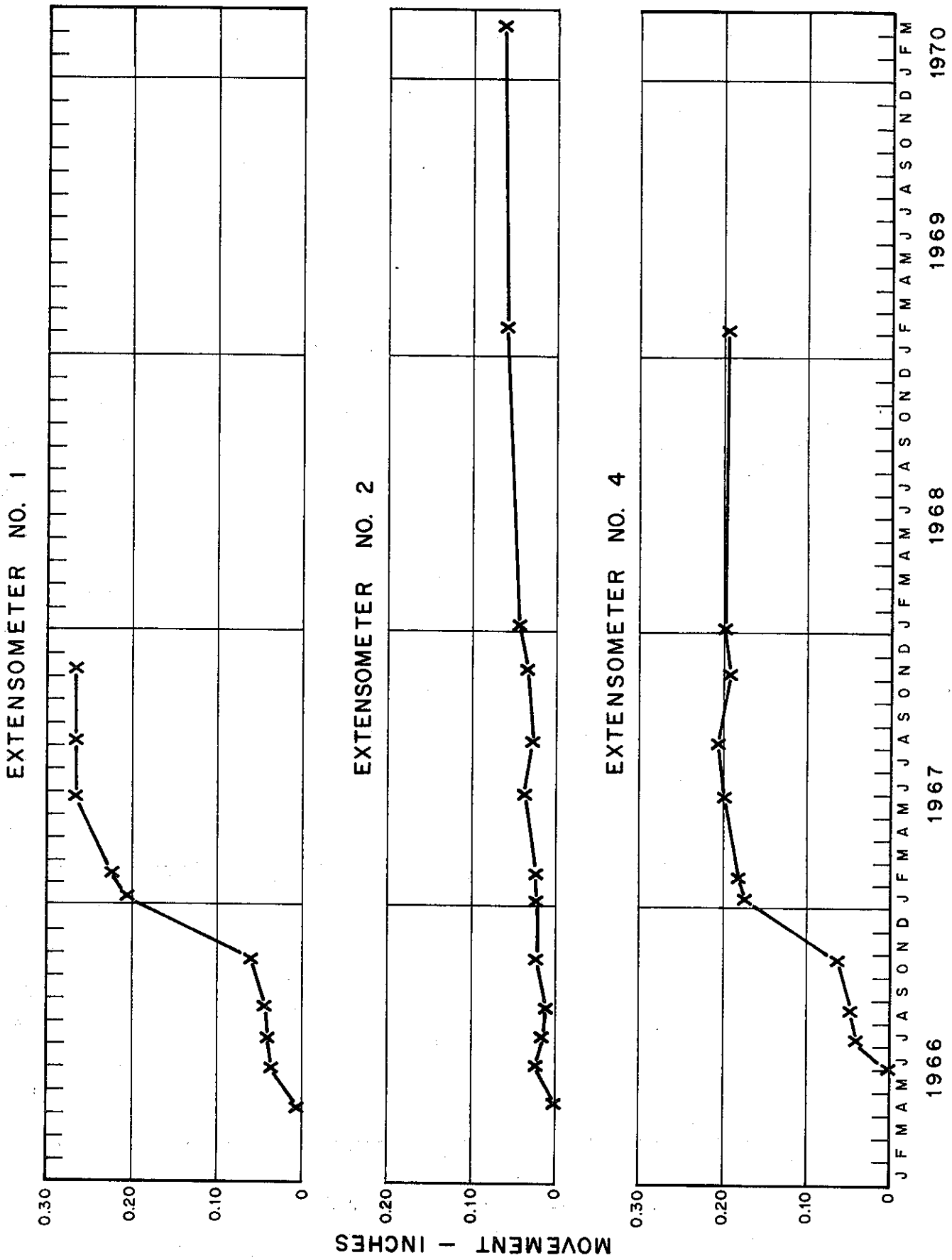

Figure 7

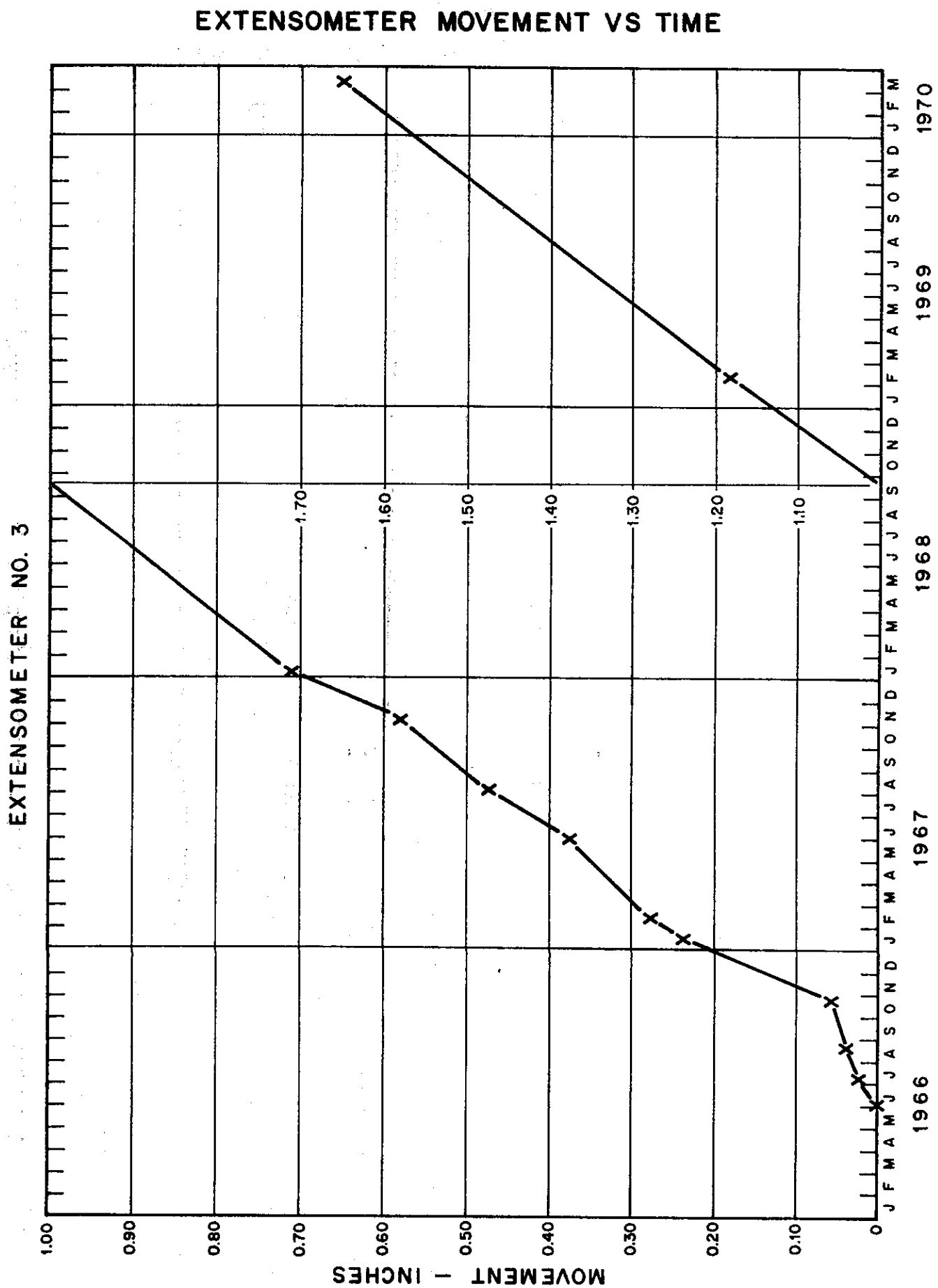

Figure 8

EXTENSOMETER MOVEMENT VS TIME

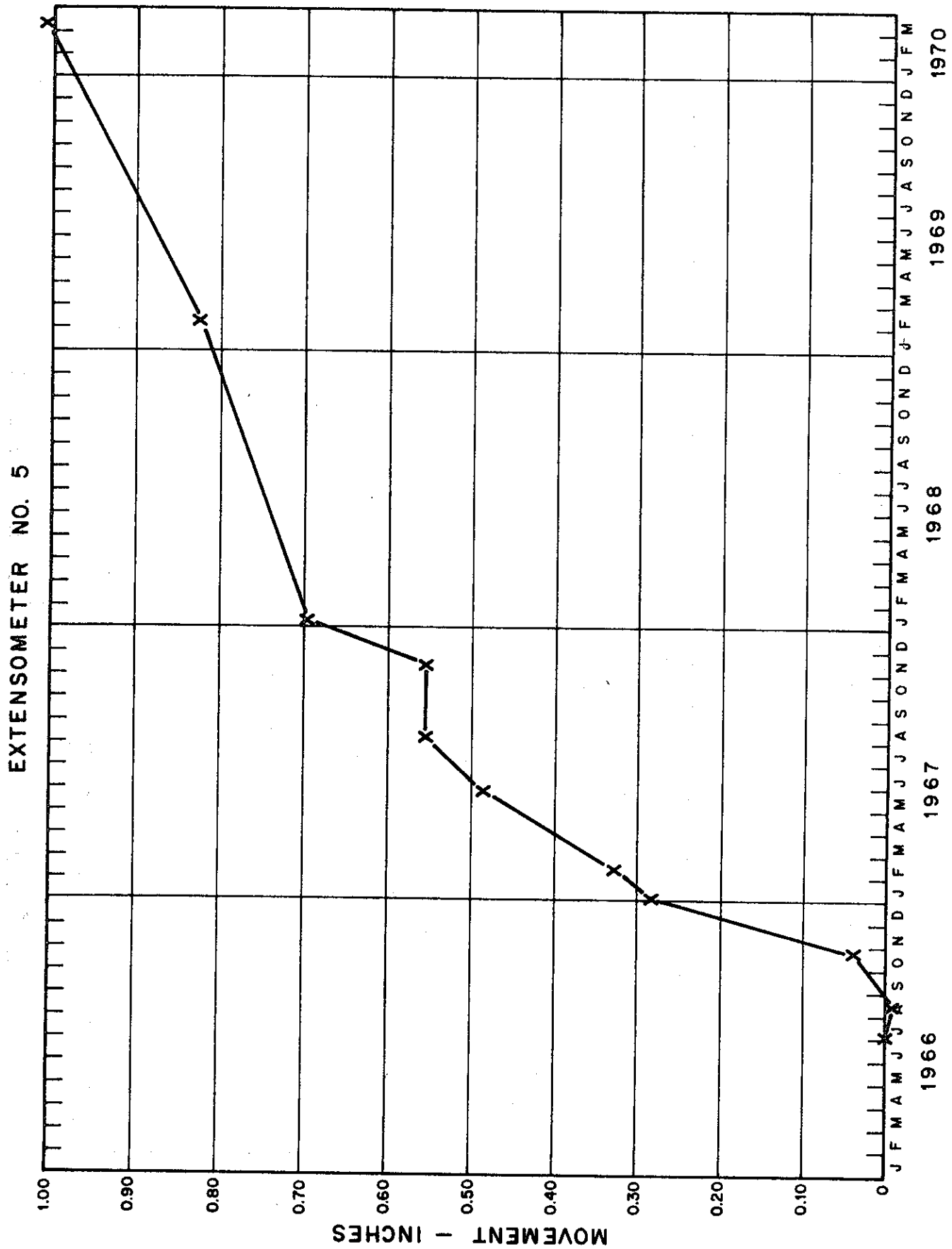

Figure 9

EXTENSOMETER MOVEMENT VS TIME

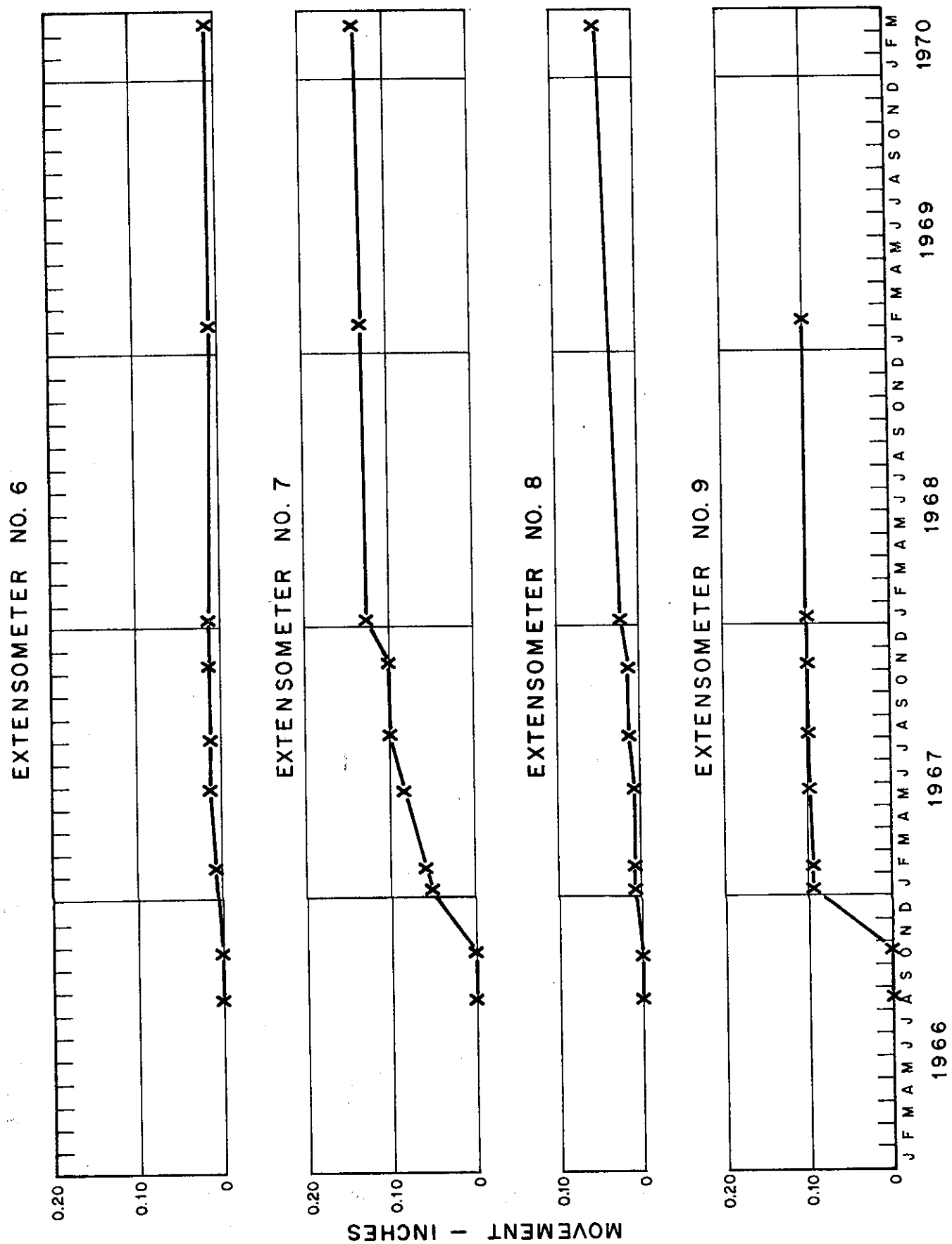

Figure 10

EXTENSOMETER MOVEMENT VS TIME

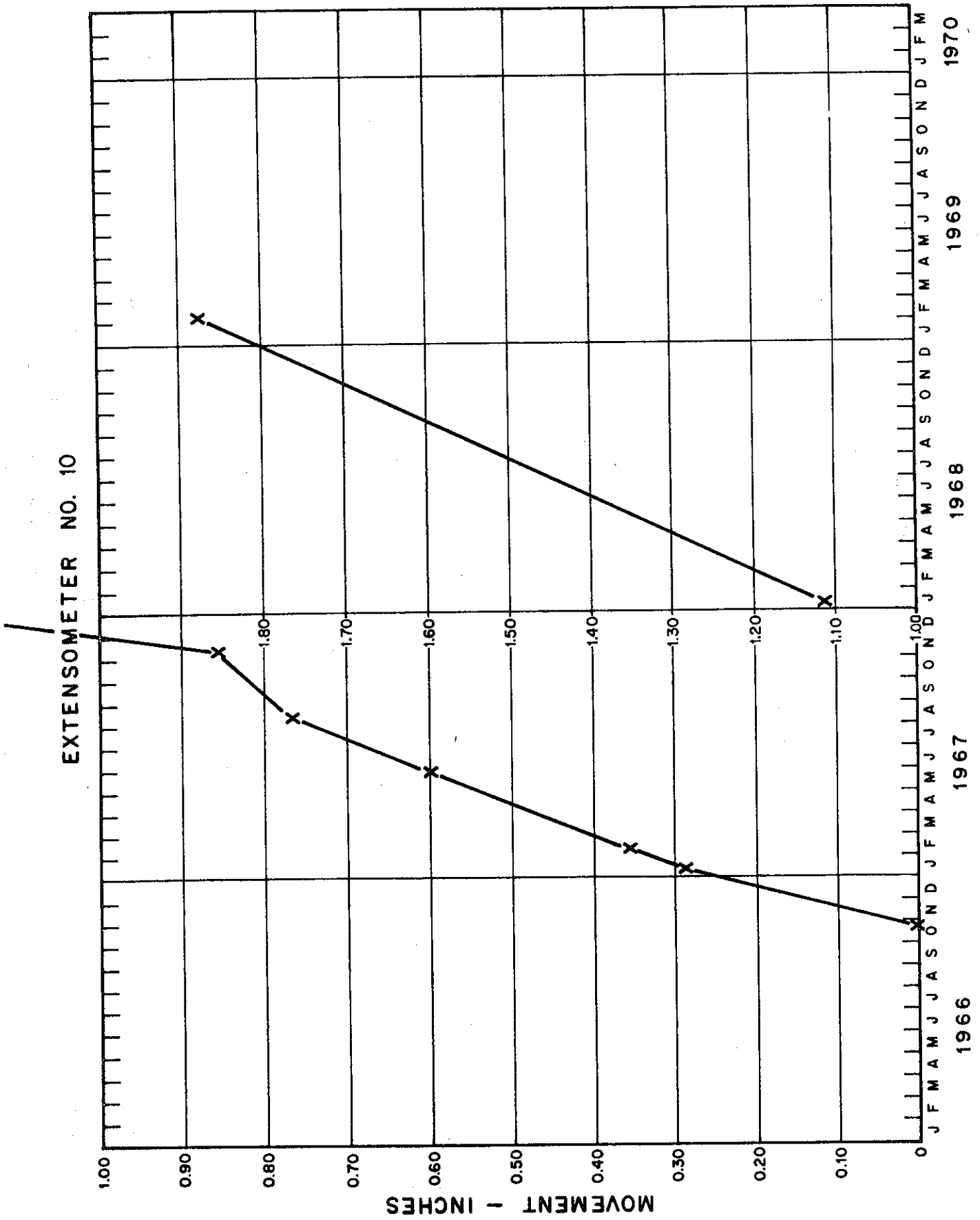

Figure 11

EXTENSOMETER MOVEMENT VS TIME

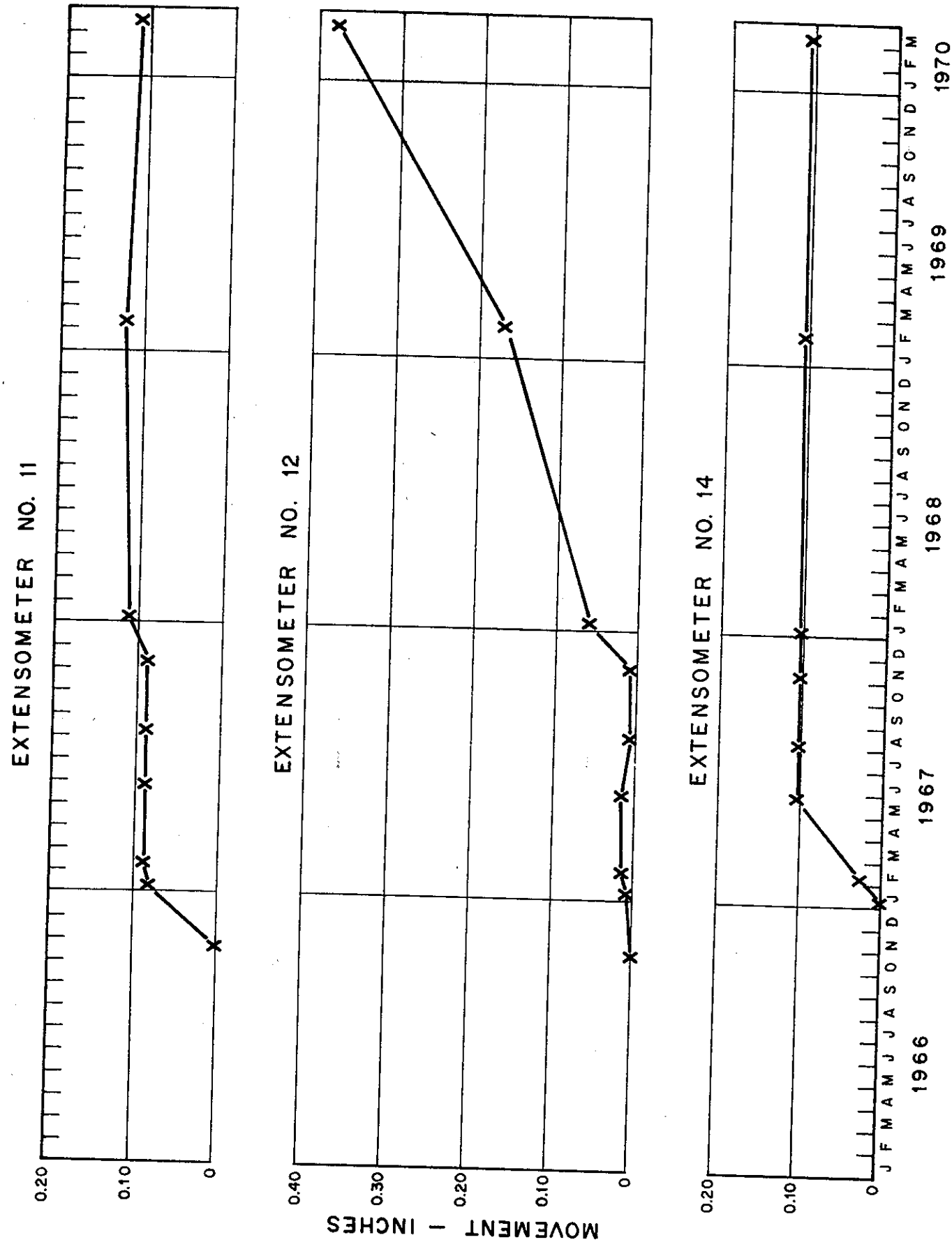

Figure 12

EXTENSOMETER MOVEMENT VS TIME

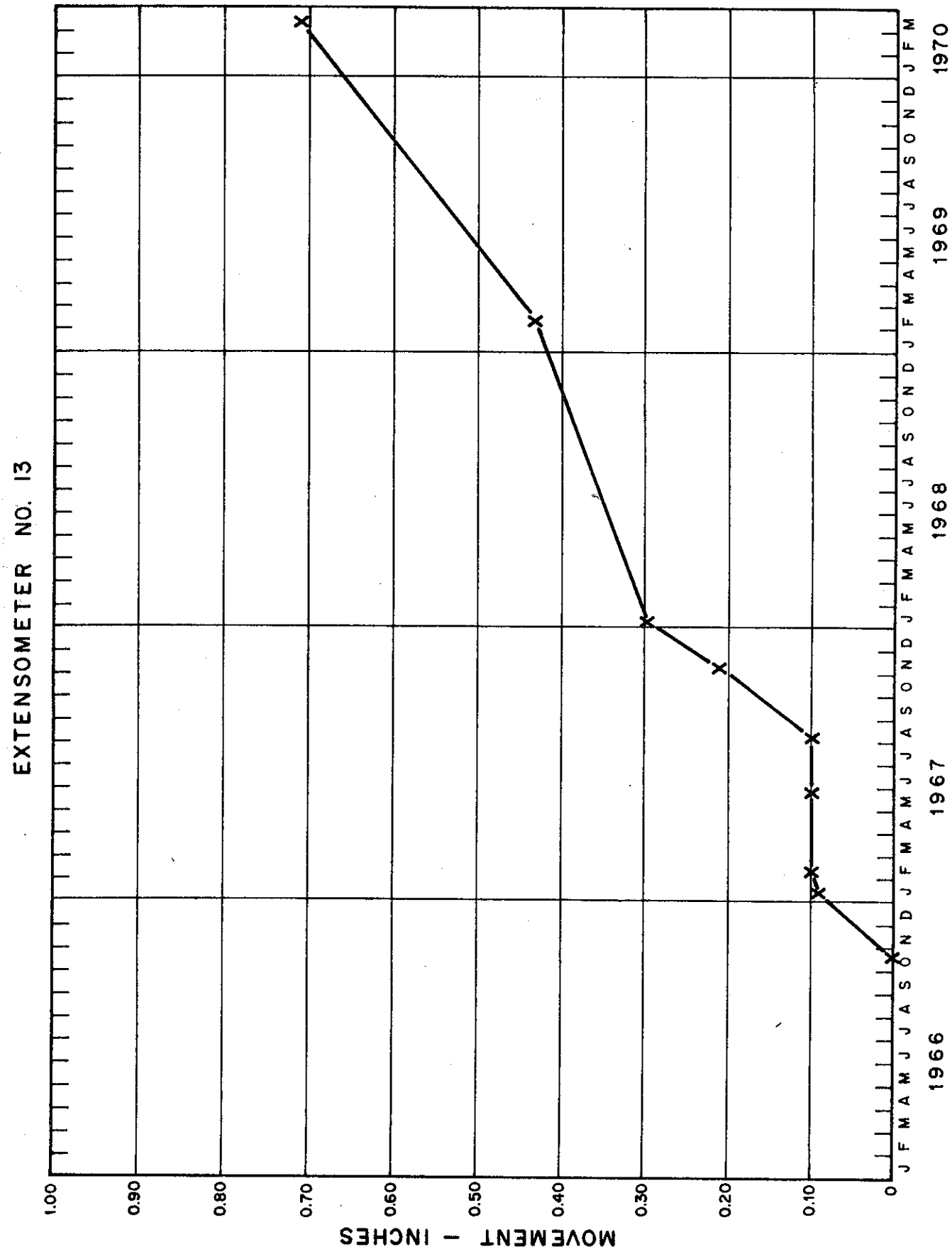

Figure 13

EXTENSOMETER MOVEMENT VS TIME

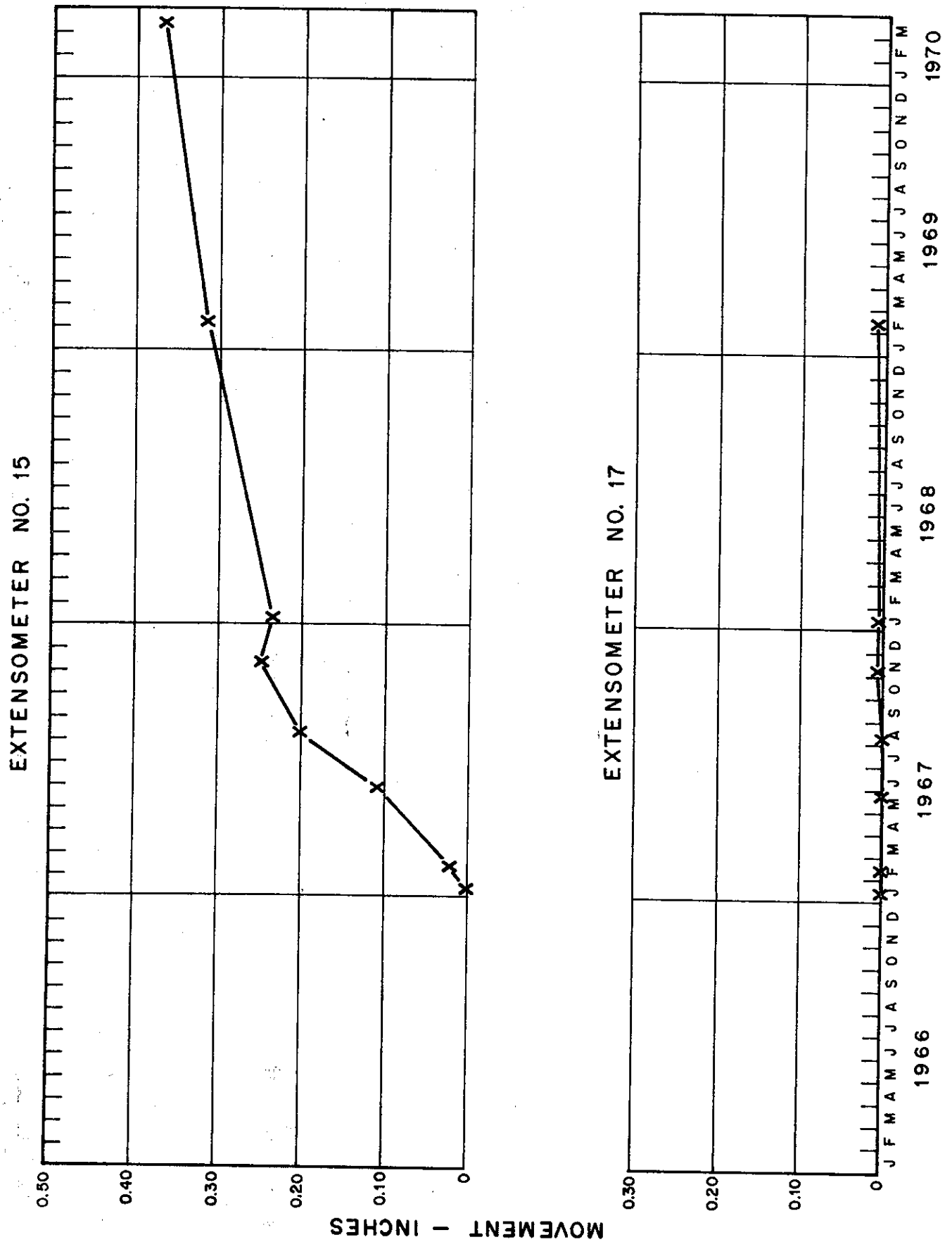

Figure 14

EXTENSOMETER MOVEMENT VS TIME

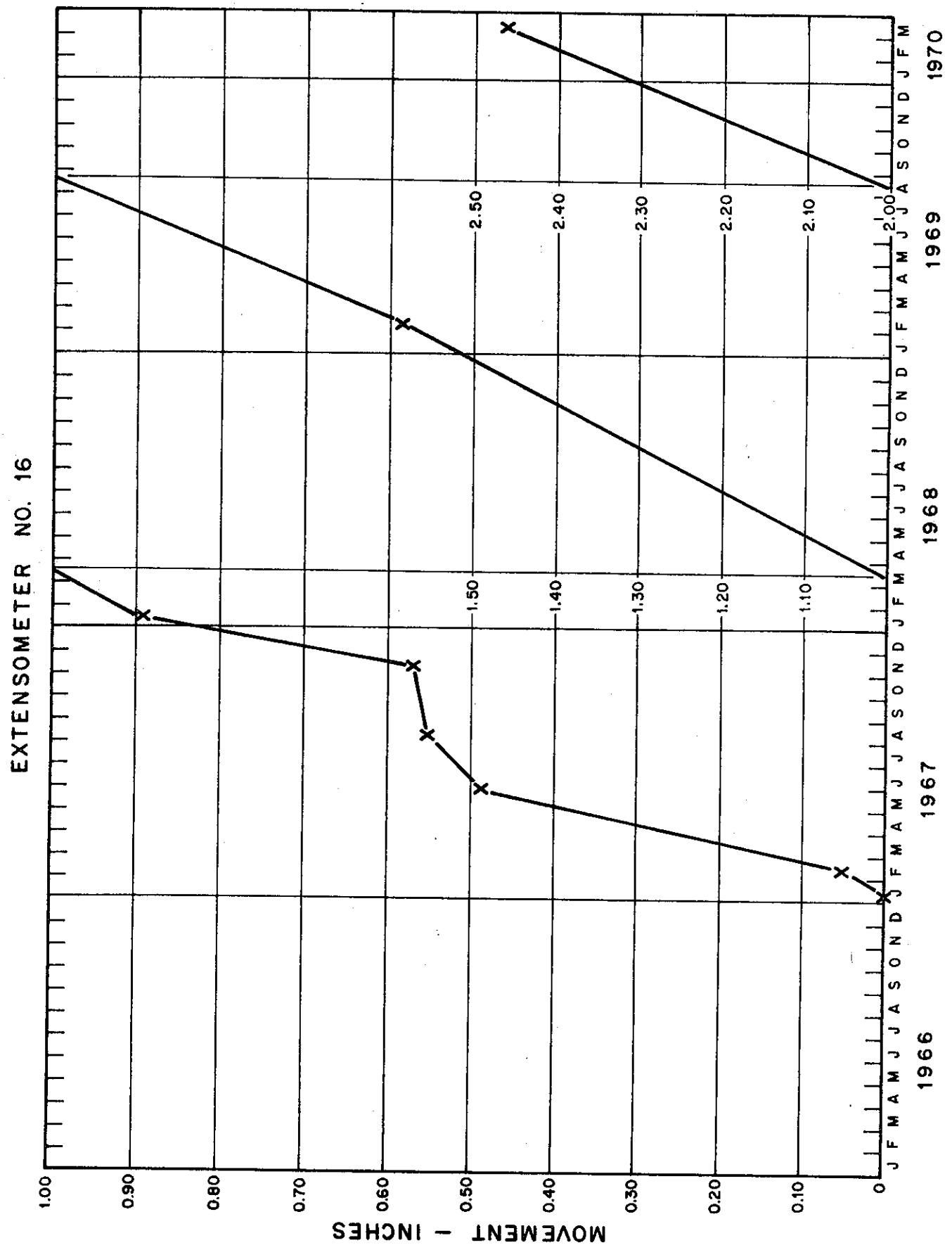

Figure 15

SCHEMATIC OF MENARD PRESSURE METER

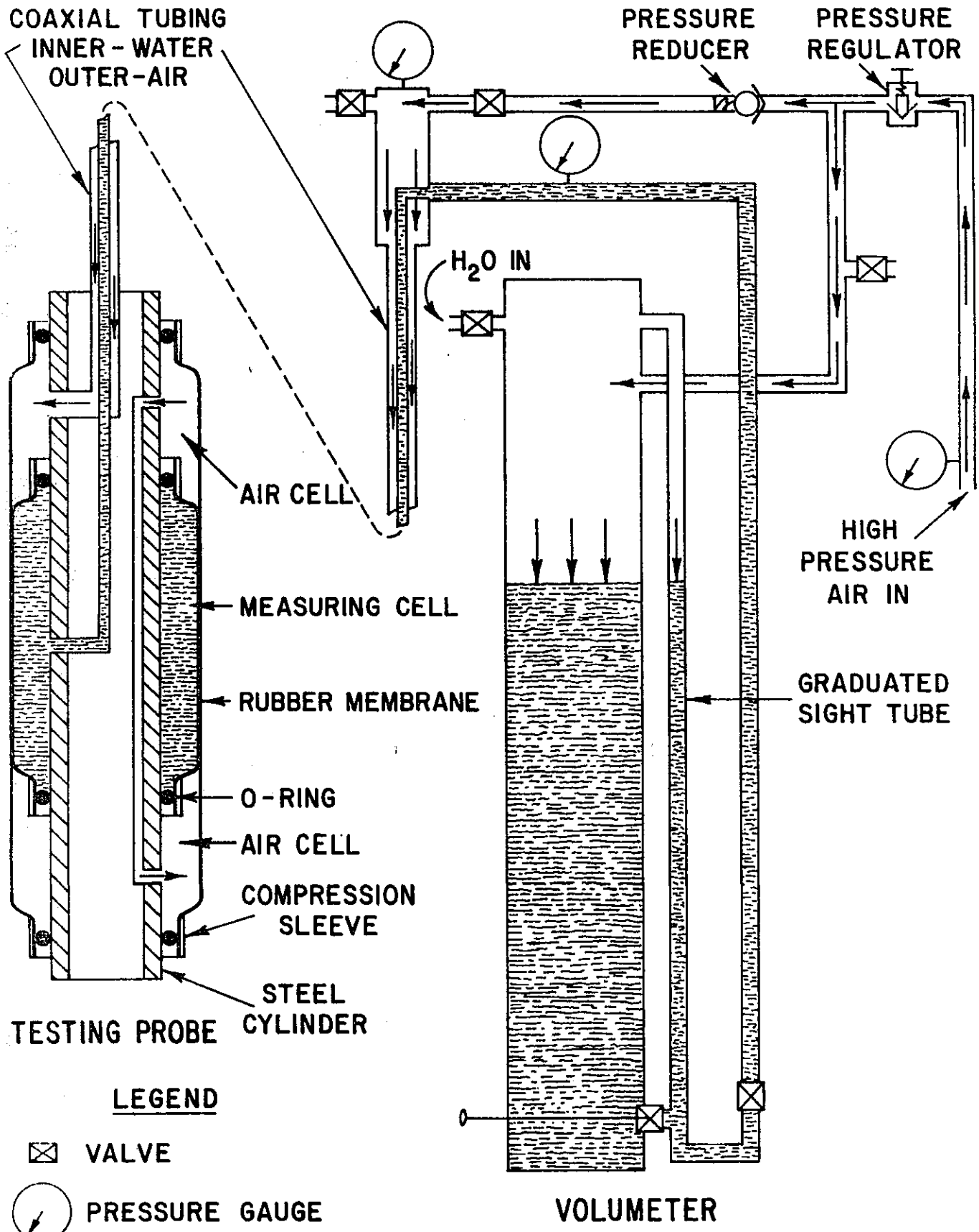

Figure 16

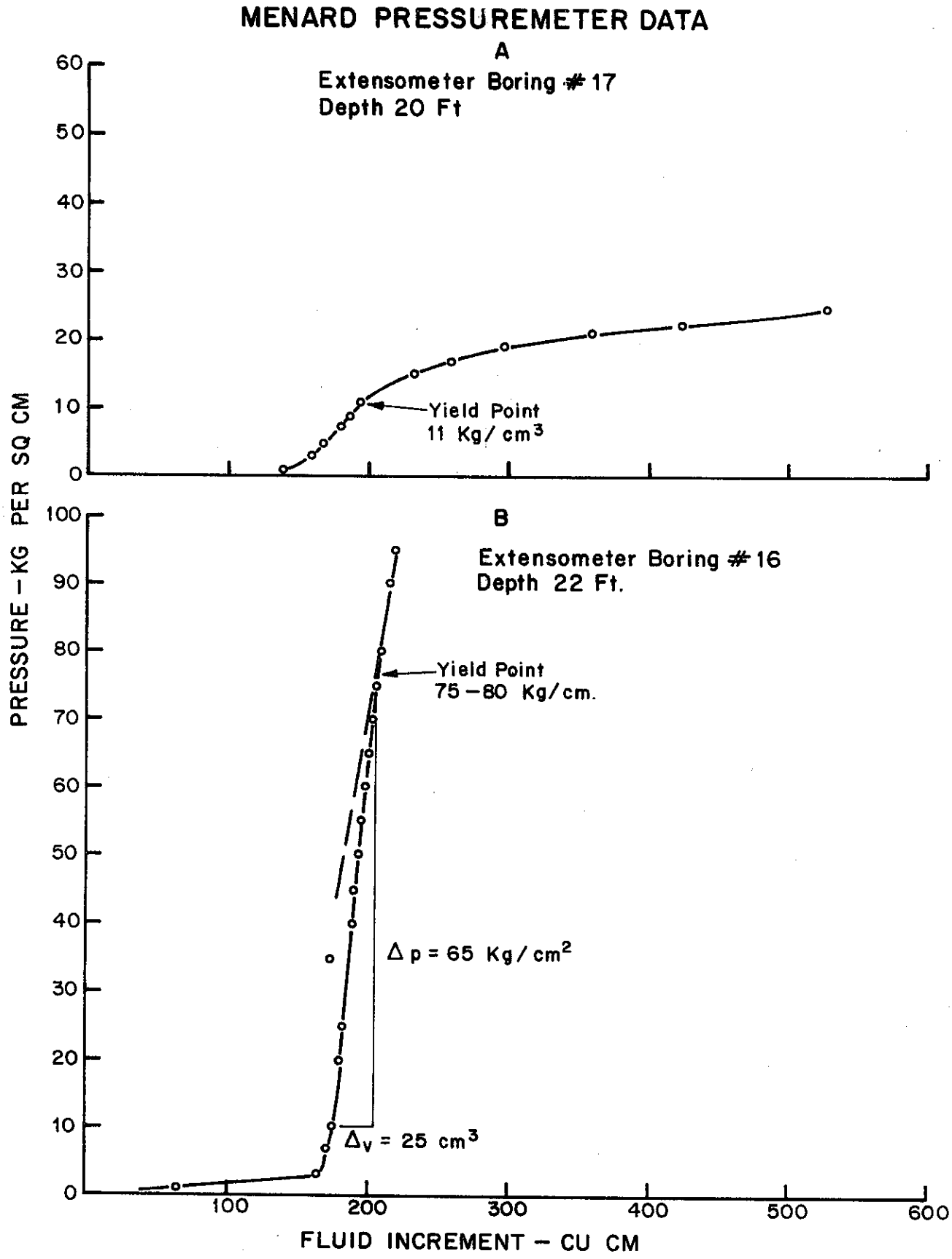

Figure 17

STRESS VS STRAIN
CONFINED CONSOLIDOMETER TESTS
(SAMPLE #8, 80'-85' DEPTH)

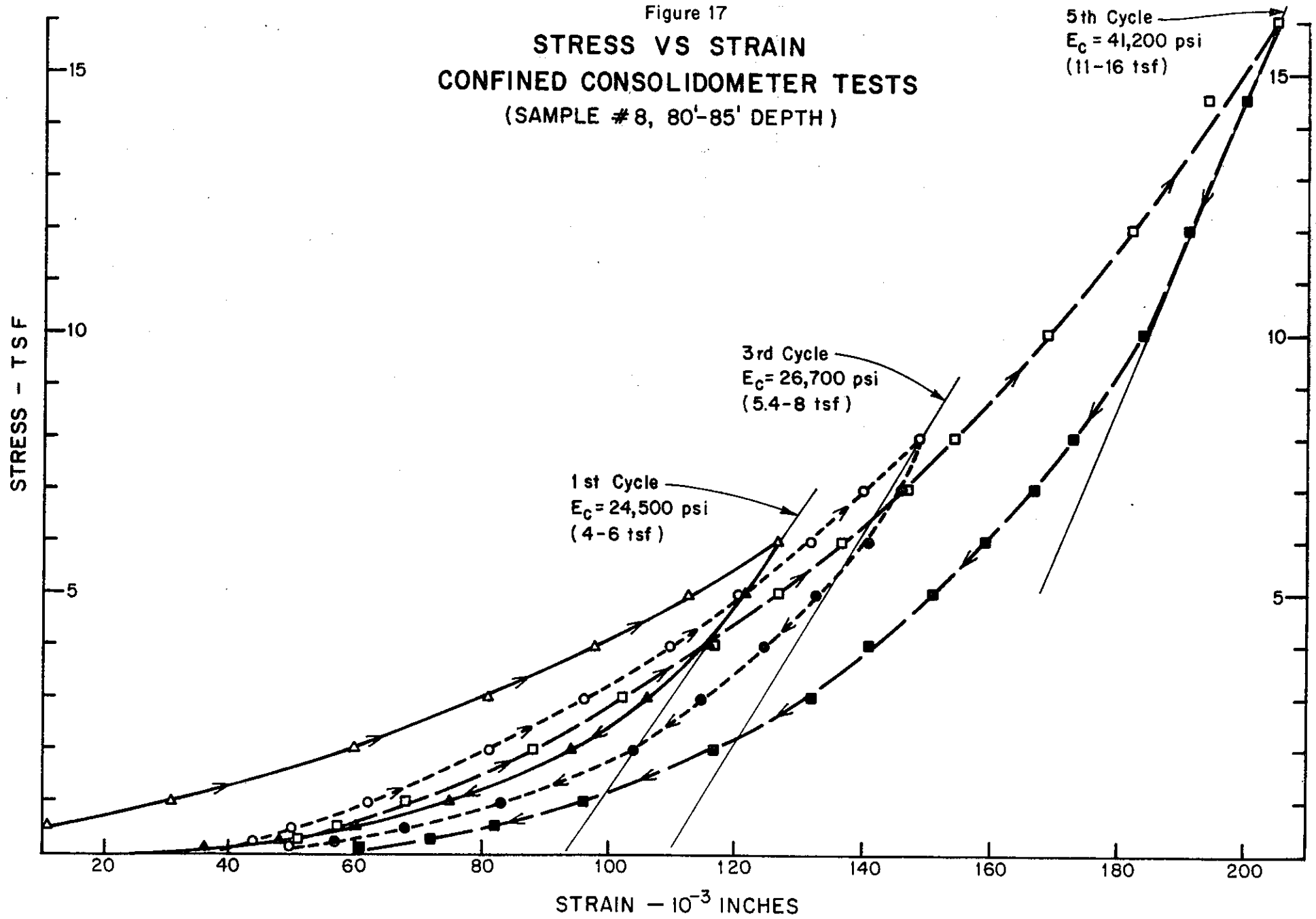

Figure 18

STRESS VS STRAIN
CONFINED AND UNCONFINED CONSOLIDOMETER TESTS
(SAMPLE # 26, 170'–175' DEPTH)

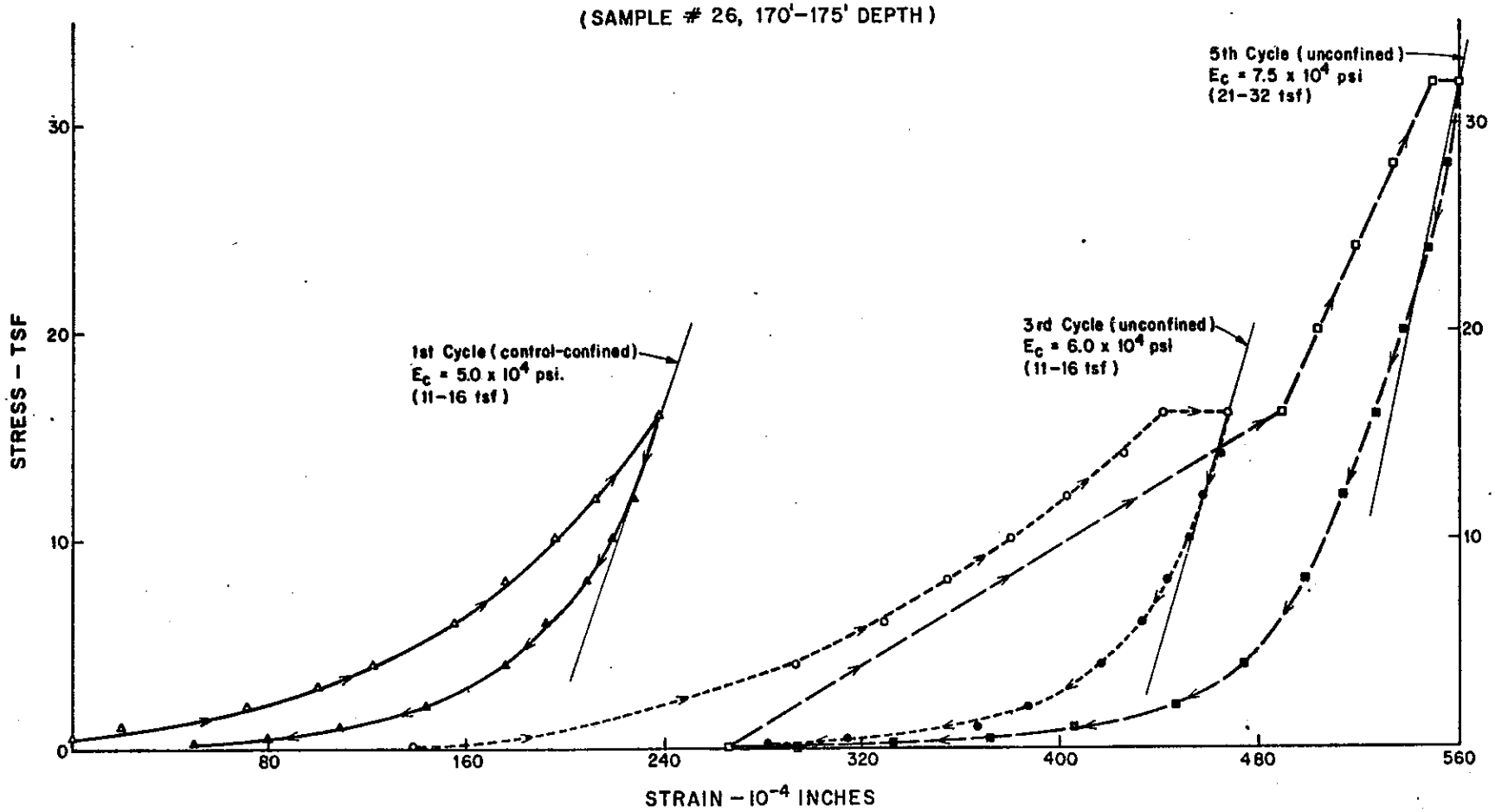

Figure 19

STRESS VS STRAIN
HIGH STRESS UNCONFINED COMPRESSION TESTS

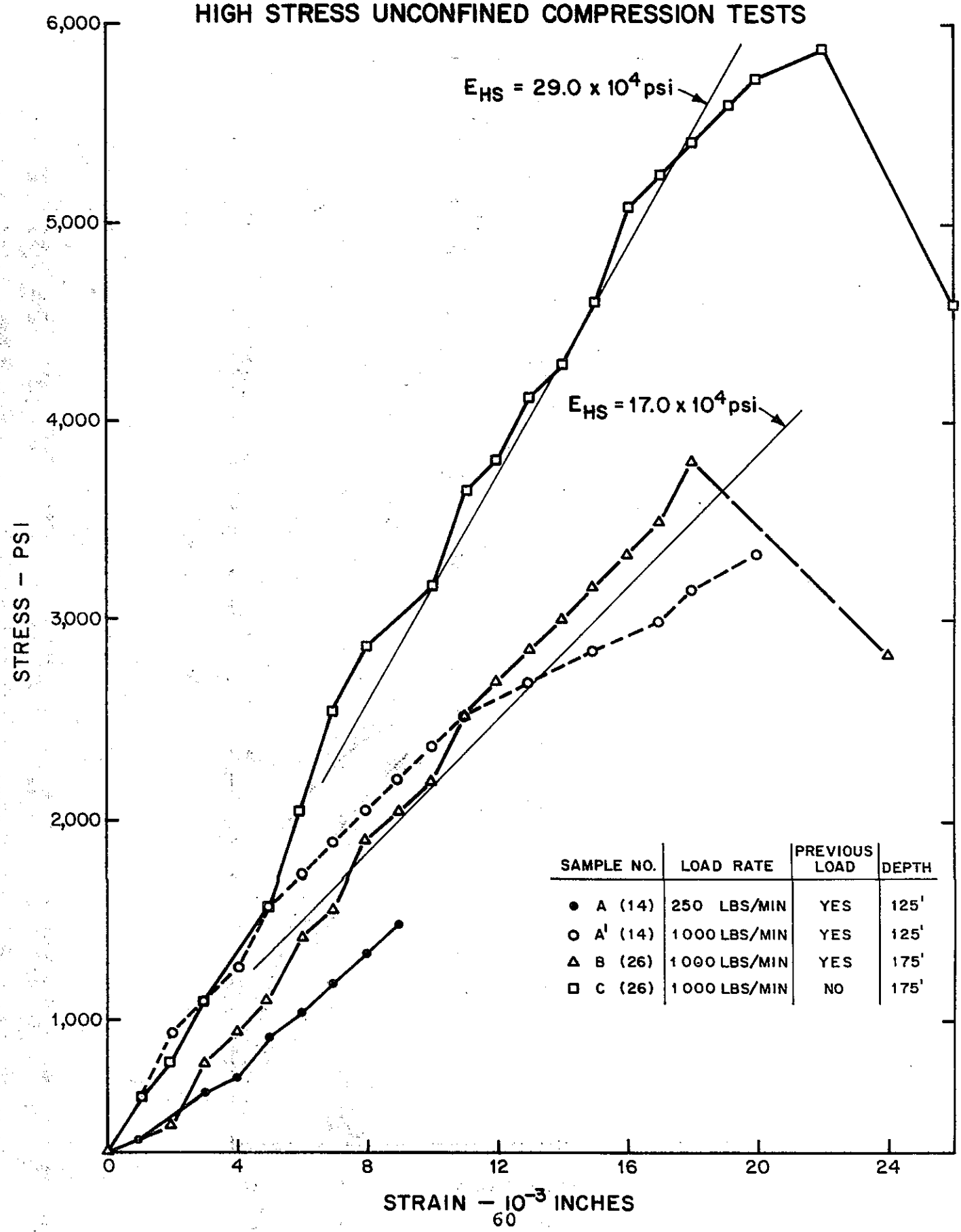

SAMPLE NO.	LOAD RATE	PREVIOUS LOAD	DEPTH
● A (14)	250 LBS/MIN	YES	125'
○ A' (14)	1000 LBS/MIN	YES	125'
△ B (26)	1000 LBS/MIN	YES	175'
□ C (26)	1000 LBS/MIN	NO	175'

Figure 20

MODULI VS PEAK STRESS

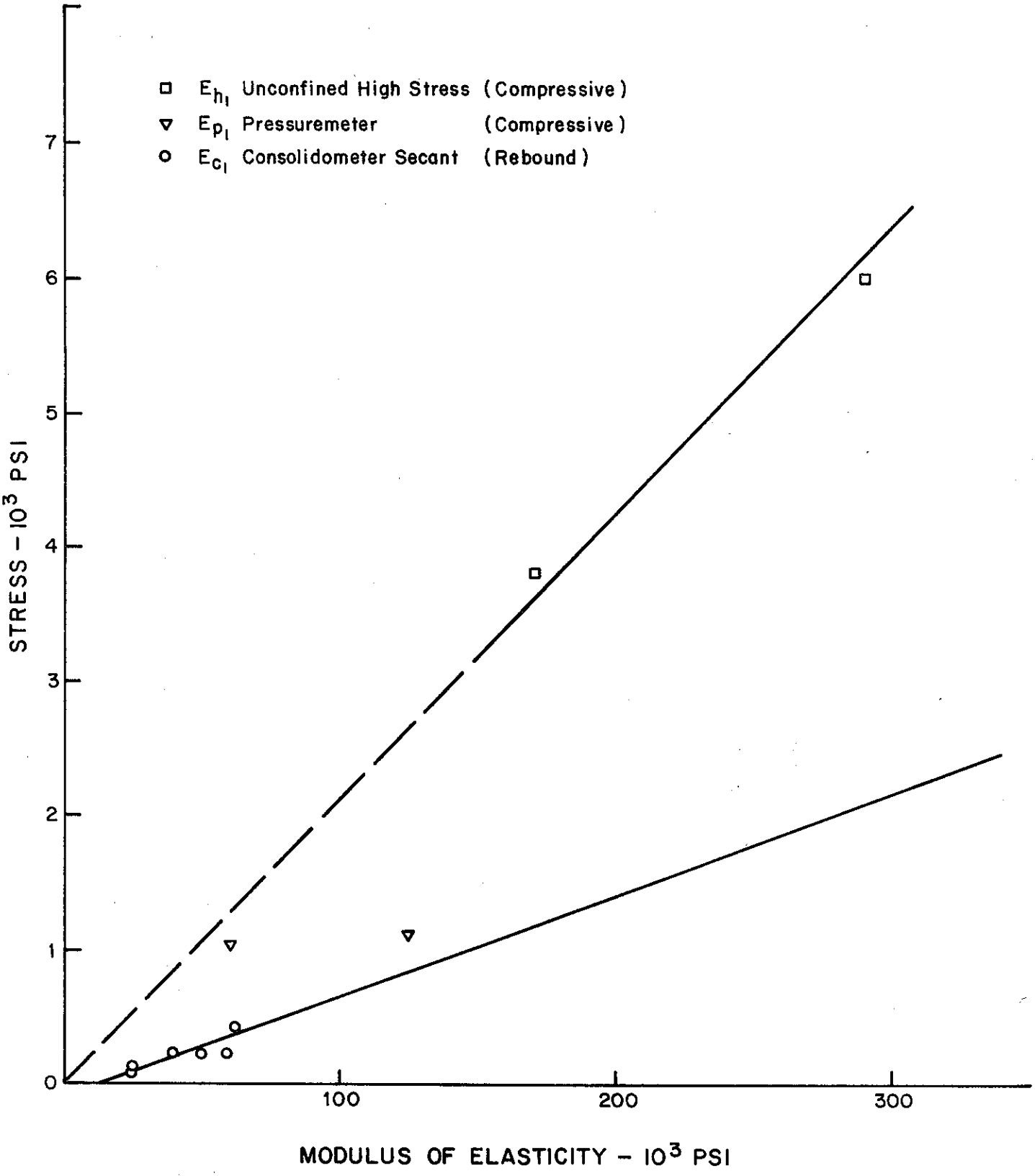

Figure 21

ACTUAL AND ASSUMED EXCAVATION LIMITS FOR FINITE ELEMENT ANALYSIS OF REBOUND

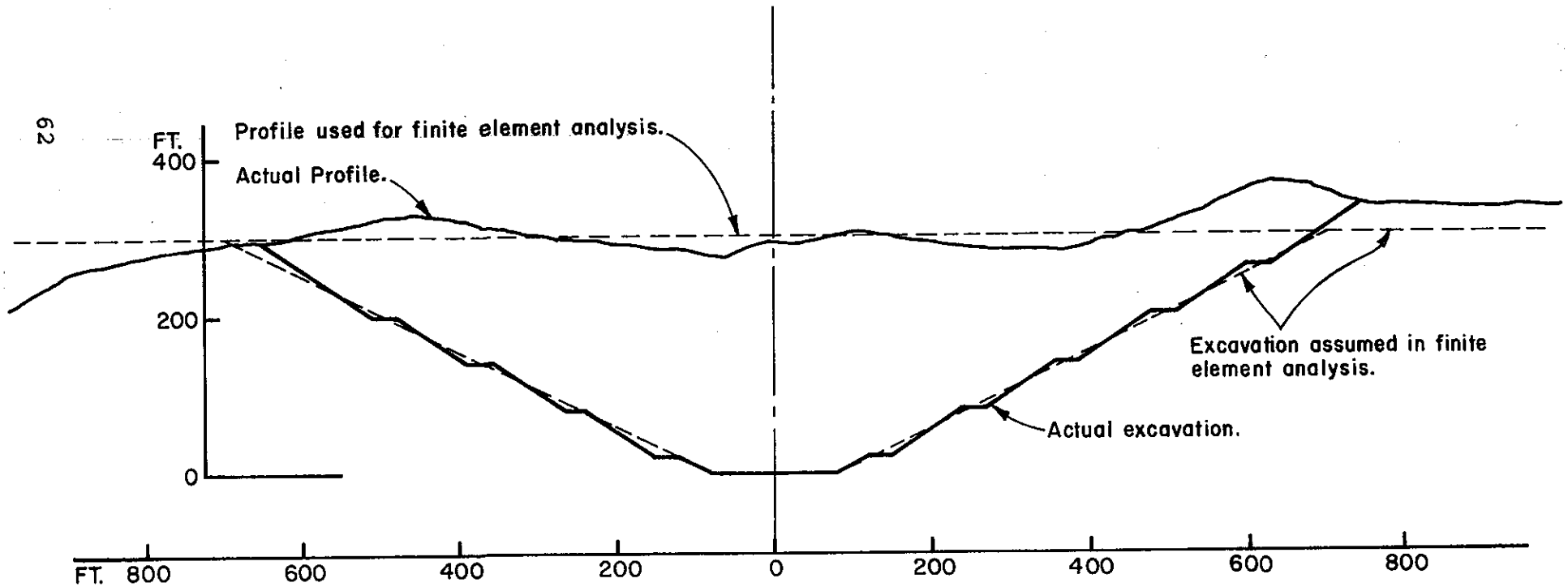

Figure 22

BOUNDARIES ASSUMED IN THE FINITE ELEMENT ANALYSIS OF REBOUND

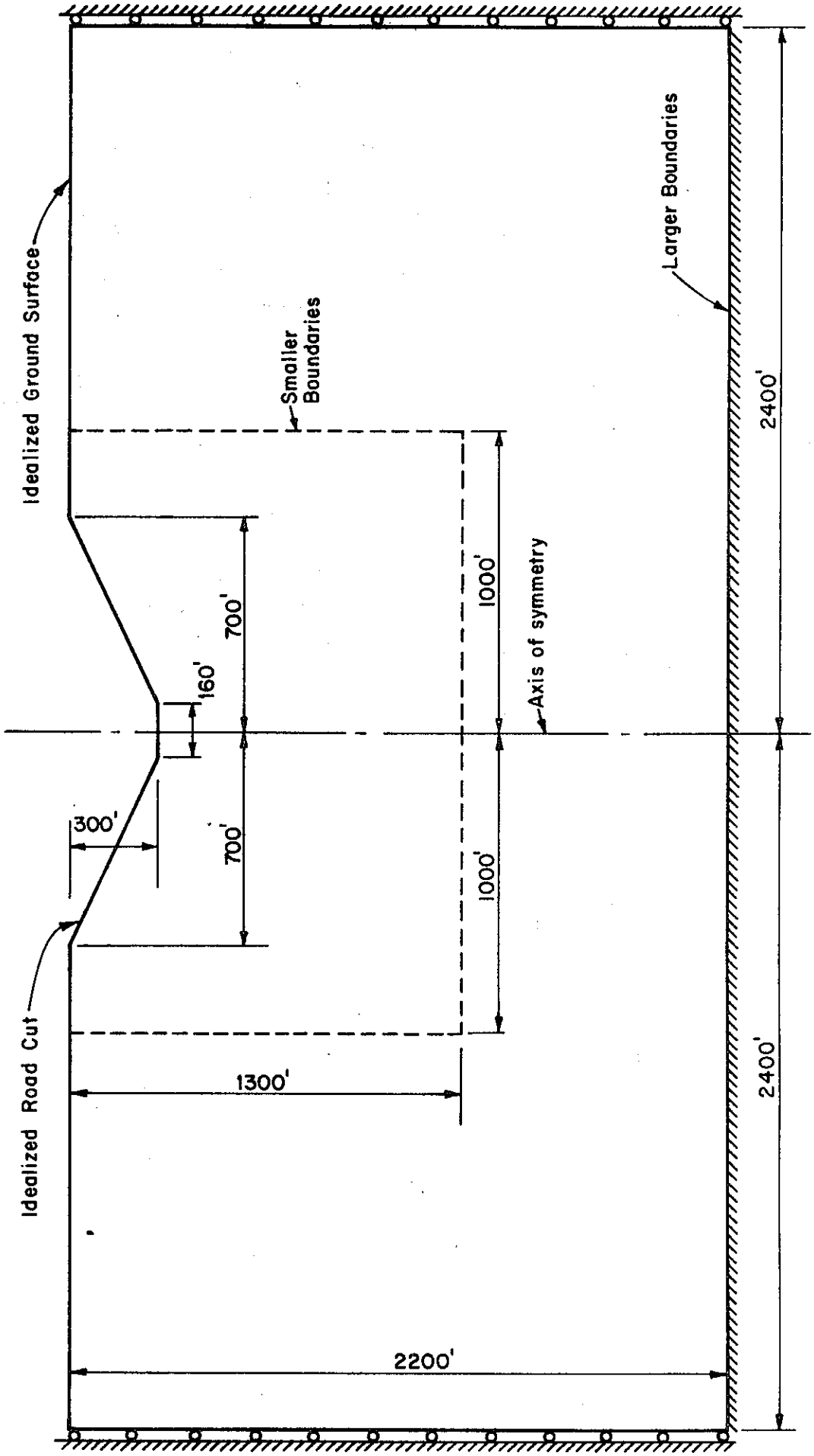

WESTERGAARD STRESS DISTRIBUTION FOR LONG CONTINUOUS LOAD

APPROXIMATE CROSS SECTION OF HIGHWAY CUT
(First Model)

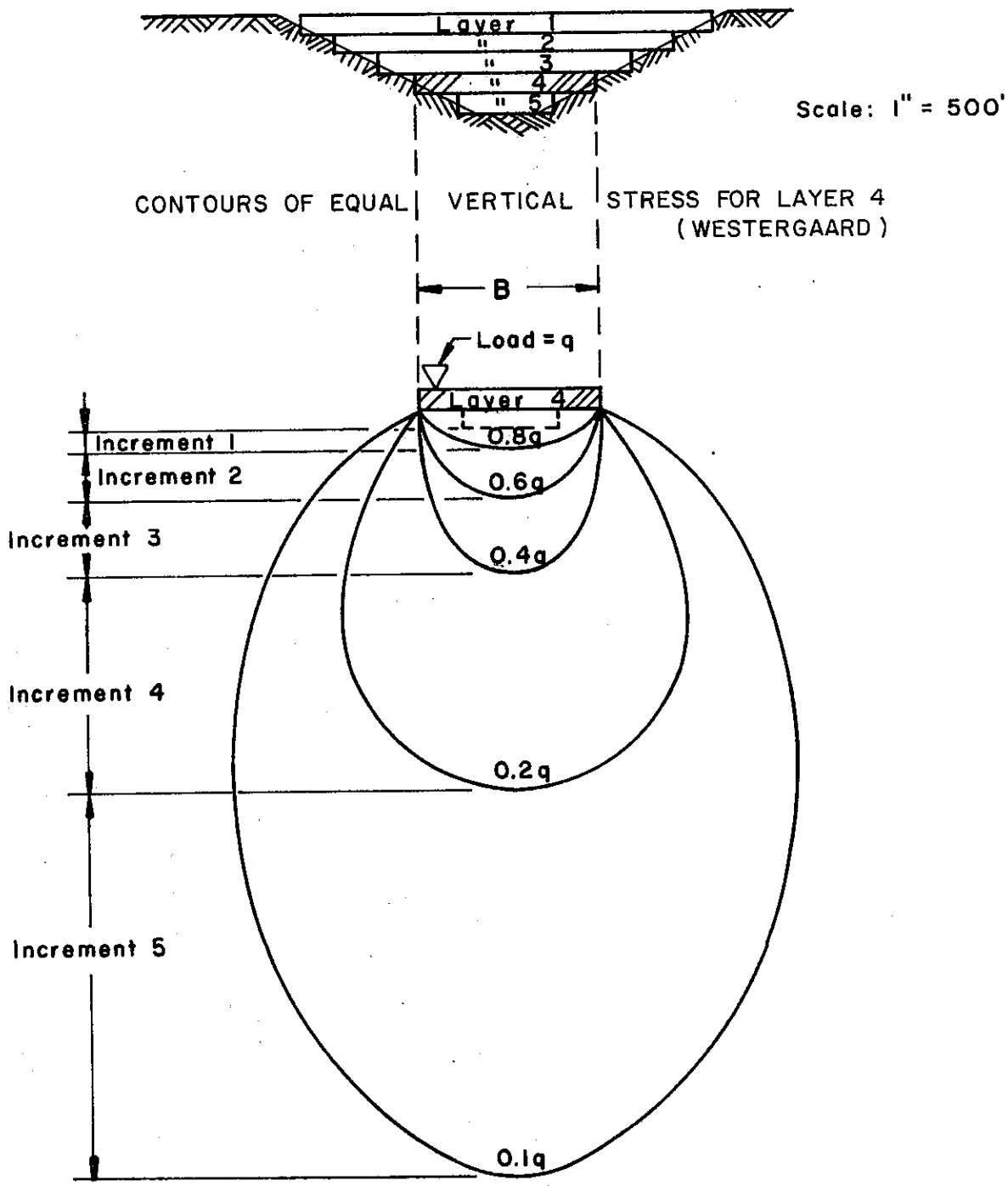

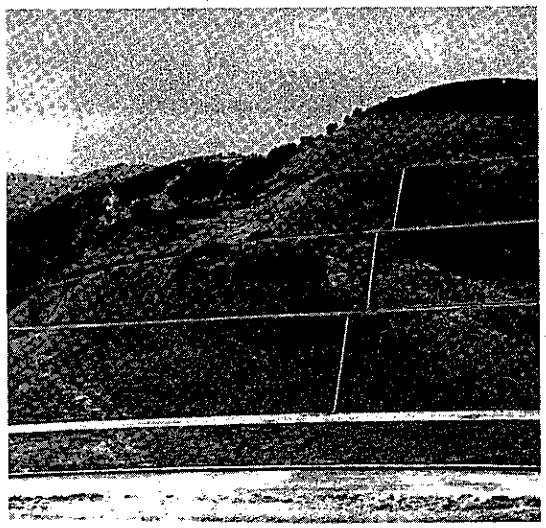

PHOTO 1

Westerly face of cut Nov. 1967,
9 months after completion.

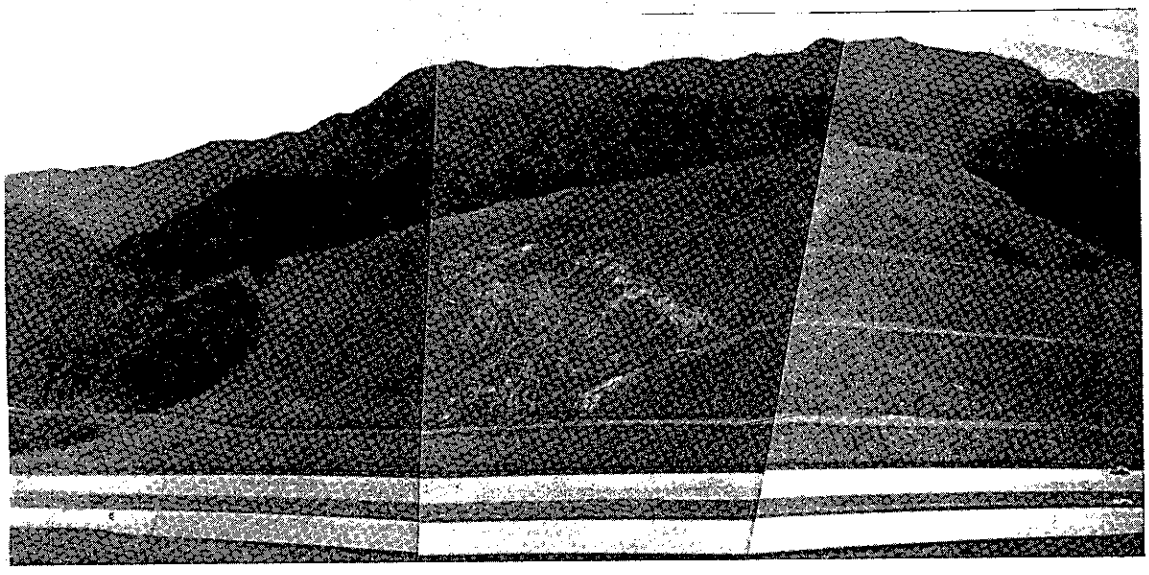

PHOTO 2

Westerly face of cut Mar. 1970,
(Perspective is from the south.)

PHOTO 3

Recovery of extended bench mark.

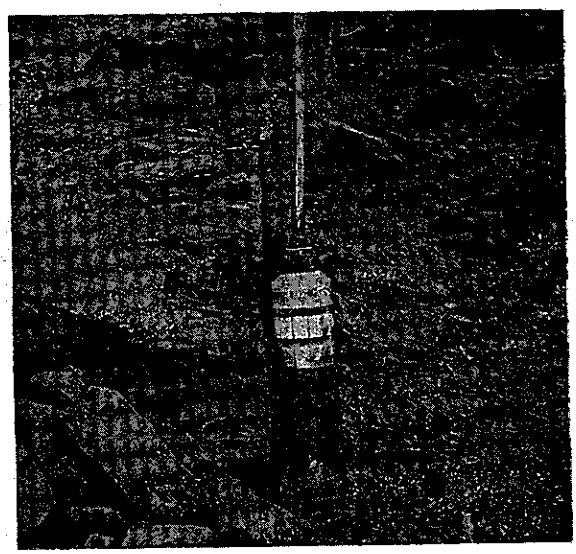

PHOTO 4

Close-up of upper bench mark at time of recovery.

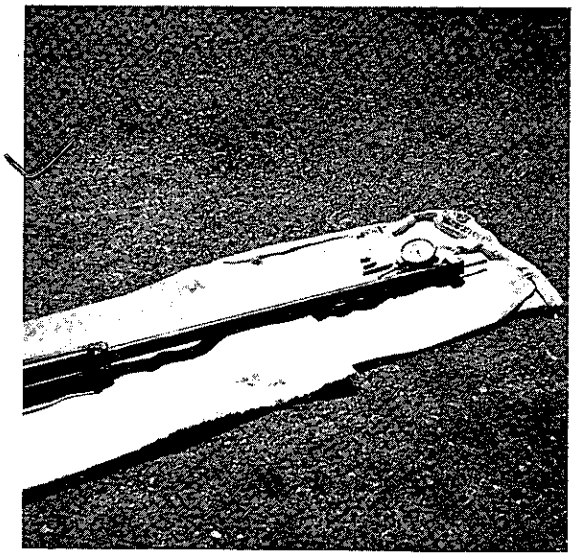

PHOTO 5

Exposed end of extensometer with dial gage in reading position.

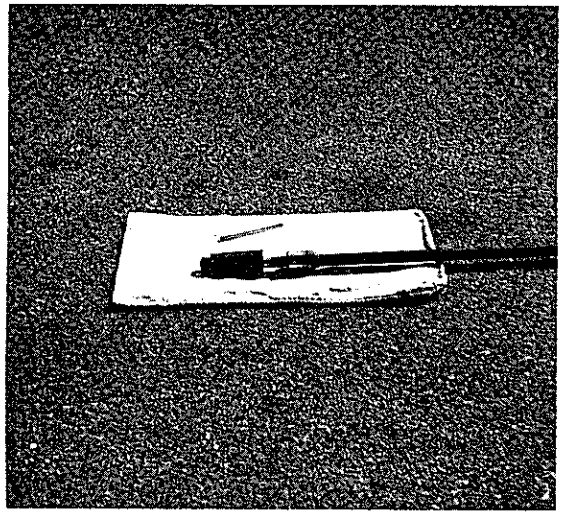

PHOTO 6

Anchor end of extensometer made from rock bolt.